Submitted to the JOURNAL OF CHEMICAL PHYSICS

LBL-8052 c.2
Preprint

LA
RCO
OSTI
CDL

VIBRATIONAL RELAXATION OF MATRIX-ISOLATED HCl AND DCl

Jay M. Wiesenfeld and C. Bradley Moore

RECEIVED
LAWRENCE
BERKELEY LABORATORY

SEP 25 1978

LIBRARY AND
DOCUMENTS SECTION

August 1978

Prepared for the U. S. Department of Energy
under Contract W-7405-ENG-48

TWO-WEEK LOAN COPY

This is a Library Circulating Copy which may be borrowed for two weeks. For a personal retention copy, call Tech. Info. Division, Ext. 6782

LBL-8052 c.2

DISCLAIMER

This document was prepared as an account of work sponsored by the United States Government. While this document is believed to contain correct information, neither the United States Government nor any agency thereof, nor the Regents of the University of California, nor any of their employees, makes any warranty, express or implied, or assumes any legal responsibility for the accuracy, completeness, or usefulness of any information, apparatus, product, or process disclosed, or represents that its use would not infringe privately owned rights. Reference herein to any specific commercial product, process, or service by its trade name, trademark, manufacturer, or otherwise, does not necessarily constitute or imply its endorsement, recommendation, or favoring by the United States Government or any agency thereof, or the Regents of the University of California. The views and opinions of authors expressed herein do not necessarily state or reflect those of the United States Government or any agency thereof or the Regents of the University of California.

Vibrational relaxation of matrix-isolated HCl and DCl

Jay M. Wiesenfeld[a] and C. Bradley Moore

Department of Chemistry, University of California
and Materials and Molecular Research Division of
the Lawrence Berkeley Laboratory, Berkeley, CA 94720

[a] NSF Predoctoral Fellow. Present address:
Bell Laboratories, Holmdel, N.J. 07733

(Abstract:)

Using infrared laser-excited vibrational fluorescence, lifetimes have been measured for HCl (v=1,2) in Ar as a function of concentration and temperature, and for dilute samples of DCl (v=2) in Ar as a function of temperature. For dilute samples at 9 K, the non-radiative decay rates/are (sec^{-1}) $(8.1 \pm 0.7) \times 10^2$ and $(3.8 \pm 0.4) \times 10^3$ for HCl (v=1,2), and $(1.2 \pm 0.2) \times 10^2$ for DCl (v=2), respectively (the DCl decay may be partially radiative). These rates increase slightly (less than a factor of 2) between 9 and 21 K. The results are consistent with a relaxation process in which the rate-determining step is intramolecular V→R transfer. No fluorescence signal is observed upon excitation of the overtone of the HCl dimer in Ar implying that relaxation of the dimer is faster than 0.3 μs. In concentrated samples the relaxation rate for HCl (v=1) (but not v=2) increases, due to energy-migration aided V→V transfer to dimers, which are an energy sink. It is argued that this system belongs to the "fast migration" regime. In N_2 and O_2 matrices, there is no fluorescence following excitation of HCl (v=2), presumably due to rapid V→V transfer to the host. Spectroscopic measurements of overtone absorption transitions are reported. A measurement of the integrated absorption coefficient for HCl in Ar indicates that the transition dipole moment differs less than 9% from the gas phase value.

I. INTRODUCTION

Studies of vibrational relaxation and energy transfer in simple condensed phase systems are beginning to yield many interesting results.[1] A variety of processes may follow vibrational excitation of a diatomic or the lowest energy mode of a polyatomic guest species in a simple solid host: 1) the molecular vibration may relax by radiative decay; 2) the vibration may relax by coupling with delocalized lattice phonons (V→P); 3) the vibration may relax into modes localized at the lattice site of the guest, such as guest rotation (V→R); 4) vibrational energy may be resonantly transferred from one guest molecule to another leading to energy migration; 5) the excitation may be non-resonantly transferred to a chemically different guest species; and 6) a chemical reaction of the excited molecule may occur. Processes 2 and 3 are the mechanisms for vibrational relaxation of an isolated guest species and are collectively labeled V→R,P processes. Processes 4 and 5 are V→V processes.

Experimentally observed vibrational relaxation times of matrix isolated species range over several orders of magnitude. Molecules with large vibrational frequencies and large moments of inertia (hence small B constants) relax very slowly. The vibrational lifetime of CO in Ar or Ne matrices is 14 ms and energy decay is radiative.[2] Homonuclear diatomics relax even more slowly. The vibrational relaxation time of C_2^- in Kr is 288 ms,[3] and those of N_2 ($X^1\Sigma$) in solid N_2[4] and N_2 ($A^3\Sigma$)

in rare gas matrices[5] are about one second. The vibrational lifetime of N_2 in pure liquid N_2 exceeds 56 seconds.[6] Molecules with smaller moments of inertia relax more rapidly. Vibrational relaxation of OH/OD ($A^2\Sigma^+$)[7] and NH/ND ($A^3\Pi$)[8] in rare gas solids, the ν_2 mode of NH_3 in N_2,[1,9] and the ν_3 mode of CH_3F/CD_3F in Kr[10] occur on a 1-10 μs timescale. In these hydride/deuteride systems as well as in NH/ND ($X^3\Sigma$) in Ar,[11] the hydrides are observed to relax more rapidly than the deuterides. Bondybey and Brus[7,8] were led to propose that guest rotation is the accepting mode for vibrational relaxation. Legay[1] has correlated existing experimental data to this hypothesis with a good degree of success. Radiative decay competes with and can be faster than relaxation into rotation for molecules with large moments of inertia. Processes 1 and 3 appear to be more important than process 2 for vibrational relaxation in solids.

Resonant and non-resonant energy transfers (processes 4 and 5) which lead to concentration of vibrational energy on a small number of highly excited guest molecules have been reported for CO in Ar and Ne.[2] Long-range energy transfer unaided by energy migration has been reported for NH/ND ($A^3\Pi$) as the energy donor to various acceptors.[12] Pimentel and co-workers reported the first IR-induced reaction in 1960, the <u>cis</u>-<u>trans</u> isomerization of matrix-isolated HONO.[13] More recently, Ambartzumian and co-workers[14] have reported the dissociation of SF_6 in an Ar matrix following absorption of many photons at 10.6 μ. Davies et al.[15] have observed the isomerization of various isotopic forms of $Fe(CO)_4$ in an Ar matrix following excitation of the CO stretching mode.

We have studied vibrational relaxation and energy transfer processes of matrix-isolated HCl and DCl using laser-excited vibrational fluorescence. The HCl system is a particularly useful prototype. HCl is a stable molecular species of which solid solutions of known concentration can be prepared. The vibrational spectroscopy of matrix-isolated HCl and DCl has been extensively studied, both experimentally[16] and theoretically,[17] and the forces responsible for the spectral perturbations are known.[17] The HCl-Ar interaction has been well studied in the gas phase by molecular beam scattering[18] and by spectroscopic observation of the ArHCl van der Waals molecule.[19-21] A single potential function for HCl-Ar which describes many phenomena of the HCl-Ar system has been proposed.[22] Finally, vibrational relaxation of HCl by Ar in the gas phase has been studied.[23]

The present studies are performed in the ground electronic state; thus, relaxation processes involving other electronic manifolds[24] cannot occur. HCl and DCl are found to decay non-radiatively in an Ar matrix. HCl relaxes more rapidly than DCl and thus dominance of the V→R relaxation process is inferred. The concentration dependence of the relaxation rate of HCl (v=1) in Ar is due to energy migration and non-resonant V→V transfer to the HCl dimer, which relaxes much more rapidly than the monomer.

The experimental techniques for matrix preparation, spectroscopy, and fluorescence studies are presented in Section II. The spectroscopy and energy level structure of

matrix-isolated HCl and DCl are treated in Section III. Kinetic results for HCl in Ar, N_2, and O_2 matrices and preliminary results for DCl in Ar are presented in Section IV. The results are interpreted in Section V in terms of V→R relaxation, and the concentration dependence of the v=1 relaxation rate is analyzed.

II. EXPERIMENTAL

A. Matrix isolation techniques

Matrices were prepared using a pulsed deposition technique under a variety of conditions: either two or four pulse/min at an average deposition rate of 5-30 m-moles/hr (total matrix), and at deposition temperatures between 9 and 20 K. Argon matrices of HCl prepared by pulsed deposition exhibit a greater degree of isolation (less polymer) than matrices prepared by continuous deposition at the same average rate under otherwise identical conditions,[25] in agreement with previous comparisons of pulsed and continuous deposition techniques.[26,27] Samples of pre-mixed gas were deposited onto a sapphire window mounted on a closed-cycle helium refrigerator (Air Products, Displex CSA-202) capable of cooling to 9.1 ± 0.3 K. Temperatures were measured to an accuracy of 0.3 K with an iron-doped gold (0.7 at. %) vs KP thermocouple which was calibrated against a hydrogen vapor pressure thermometer in the range 14-22 K. Temperatures above 9 K were maintained by passing a dc current through a resistive heater wrapped around the cold station.

Gas mixtures were prepared on a mercury diffusion pumped, greased vacuum line, capable of producing a vacuum better than 1×10^{-6} Torr, and having a combined outgassing-leak rate of less than 2×10^{-5} Torr/hr. Since HCl adsorbs slightly on glass walls, the 5 ℓ sample bulbs were flamed before use and HCl pressures were equilibrated before addition of the matrix gas. Gas mixtures were allowed to stand at least eight hours before use to ensure complete mixing. The mole ratio in the

matrix was assumed to be the same as the gas mixture. Pressures were measured with a mercury triple-McLeod gauge and a mercury manometer with accuracies of better than 2%.

DCl was prepared by photochemical reaction of D_2 and Cl_2 in excess D_2. The Cl_2 is entirely consumed by the reaction and the excess D_2 removed by distillation. Other gases used were: HCl (Matheson Electronic Grade, > 99.99%), D_2 (Matheson CP, > 99.5% d, < 0.03% non-hydrogen impurities), Cl_2 (Matheson Research Purity, > 99.96%), CO (Matheson Research Purity, > 99.99%), Ar (Matheson Ultra-high Purity, > 99.9995%), N_2 (Matheson Research Purity, > 99.9995%), and O_2 (Matheson Research Purity, > 99.99%). HCl and DCl were distilled at least once between an isopentane-n-pentane slush (139 K) and liquid nitrogen. Before preparing a matrix sample, the HCl and DCl were subjected to at least one freeze-pump-thaw cycle. Ar, N_2, and O_2 were withdrawn from a bulb with a cold finger immersed for several hours in liquid nitrogen. Occasionally, the Ar was used directly from the cylinder.

Infrared absorption spectra were recorded on a Beckman IR-12 spectrometer with a resolution of about 1 cm^{-1}. Every matrix sample studied was characterized quantatively using integrated peak absorbances, with estimated errors of 15% for 30-50% absorbing peaks, and up to 25% for weaker peaks. Overtone absorption spectra of very thick matrices were recorded on a Cary 14 spectrometer with a resolution of 3 cm^{-1} at 5600 cm^{-1}, and 1.5 cm^{-1} at 4100 cm^{-1}. The accuracy of the Cary 14 was calibrated to within 0.7 cm^{-1} at 5600 cm^{-1}

by the v=0 → v=2 absorption spectrum of gaseous HCl.[28]

B. Fluorescence experiments

The fluorescence experiments were initiated by narrow bandwidth pulses from a Nd:YAG laser-pumped optical parametric oscillator (OPO) tuned to one of the absorption lines of the guest species being studied. Vibrational fluorescence from the excited sample was detected by a photoconductive infrared detector. The post-detector electronics depended upon the particular experiment. Three types of fluorescence experiments were performed: time-resolved emission studies, emission spectroscopy, and fluorescence excitation spectroscopy. An overall schematic for the fluorescence experiments is shown in Fig. 1. The OPO and fluorescence detection equipment have been discussed previously.[29] The IR pulses had the following characteristics: at 1.8 μ, 13 μJ/pulse, 200 ns duration; at 2.4 μ, 25 μJ/pulse, 80 ns duration; at 3.5 μ, < 2 μJ/pulse, 40 ns duration; a repetition rate of up to 75 Hz; and a spectral linewidth of 0.2-0.3 cm^{-1}.[30,31] The OPO idler frequency was calibrated by single beam absorption spectroscopy on HCl or DCl to an accuracy of 1 cm^{-1}, and a repeatability of 0.3 cm^{-1}.

The infrared beam was collimated by a 25 cm focal length lens and directed into the matrix. Two excitation geometries were used. For some experiments in which the first overtone ($\Delta v = 2$) is excited, the IR beam was passed through the matrix toward the infrared detector (the final two mirrors in Fig. 1 were removed). A cooled dielectric interference filter permitted transmission of only $\Delta v=1$ transitions. In other

experiments the geometry of Fig. 1 was used. A 4 cm focal length CaF_2 lens focused the excitation to a spot size of 60-80 μ at the sample in some experiments; in other experiments the collimated beam was used (beam diameter of 260-370 μ at the sample). Typically, the strongest fundamental line of the guest was 50% absorbing, which implied one or two percent overtone absorption for HCl.[32] Sample heating following focused pulsed excitation was negligible, since the thermal decay time for Ar at 10 K is less than 7 μs,[25,34] and thus is faster than all measured vibrational relaxation times. Assuming thermal relaxation is slower than vibrational relaxation, a maximum temperature rise of 3 K is calculated for focused excitation of samples with M/A greater than 1000. Heating effects are smaller under unfocused conditions.

A 5 cm f/1 CaF_2 lens focused the fluorescence from the matrix onto a photoconductive mercury-doped germanium detector cooled to 14 K. The detector was shielded from 300 K background radiation and scattered light by a cooled (77 K) dielectric interference filter mounted inside the detector dewar. A second interference filter mounted outside the detector dewar further spectrally resolved the fluorescence; HCl $v=2 \rightarrow v=1$ fluorescence was easily resolved from $v=1 \rightarrow v=0$ fluorescence. Depending upon the signal amplifier used, the time response of the detector and the post-detector electronics was 0.4 or 10 μs.

Fluorescence decay traces were recorded with a Biomation 8100, Northern 575 signal averaging combination. Typically

500 to 10,000 shots were averaged depending upon the magnitude of the fluorescence signal. Single shot signal-to-noise ratios were as high as five when a strong absorption line was excited. The final decay traces analyzed usually had S/N ratios in excess of 30.

Lifetimes were obtained by analyzing the decay curves as single or double exponentials. Amplifier distortion and finite S/N ratios could introduce error into the analyzed lifetimes. Electronic bandwidths were chosen so that amplifier distortion introduced less than 7% error in single exponential decays.[25] For S/N ratios as low as 10, error in analyzing single exponentials is at most 10%, and this decreases for higher values of S/N. When two exponentials have nearly equal decay times, extraction of two "exact" decay times is difficult even with infinite S/N. The problem was resolved by judicious choice of IR filters so that particular decay constants were measured in decay traces of spectrally resolved and broadband fluorescence (Sec. IV). When v=1 of HCl was directly excited, an interference filter did not eliminate scattered light, since excitation and fluorescence frequencies were identical. Scattered light saturated the detector pre-amplifier which required about 100 μs recovery time. Vibrational lifetimes were measured from the long time tail of the fluorescence decay curves in these experiments.

A low resolution fluorescence spectrum was obtained using a copper-doped germanium detector with a cooled circular variable filter (CVF).[37] The CVF was scanned in 20 cm^{-1} steps, and the

fluorescence decay curve at each step was integrated. The major source of error in the emission spectrum was fluctuation (<20%) of the OPO power during the experiment. The method of analysis is discussed in Section IV.

A fluorescence excitation spectrum was produced by replacing the signal averaging electronics with a gated electrometer[38] (Fig. 1). The gate opened with the laser pulse and closed after periods up to one millisecond. The electrometer produced a dc output with S/N proportional to the product of laser pulse energy, square root of laser repetition rate, absorption coefficient at the laser frequency, and decay time of fluorescence. With a 1 cm^{-1}/min scan rate and 2 sec time constant the spectral resolution was equal to the OPO line width of 0.2-0.3 cm^{-1}. Species which had fluorescence decay times of 5-10 μs or longer should have produced observable peaks (S/N > 1).

III. SPECTROSCOPY

The spectroscopy of matrix-isolated HCl and DCl has been well studied.[16,17] The monomeric and multimeric vibration-rotation spectra of HCl and DCl in Ar are first reviewed. Then spectroscopy of non-rotating HCl in molecular matrices of N_2 and O_2 is presented. Direct spectroscopic observations of overtone absorption in some Ar and N_2 matrices are reported. Finally, the absolute absorption coefficient of HCl in an Ar matrix is reported, from which the pure radiative lifetime is deduced.

A. Spectroscopy of the fundamental region

A typical absorption spectrum of HCl in Ar is shown in Fig. 2. Accurate linewidths are more easily measured from fluorescence excitation spectra. Widths of 1.3 ± 0.2 and 2.4 ± 0.2 cm^{-1} (FWHM) at 9 and 20 K, respectively, were found for both R(0) and P(1) lines at M/A > 1000.[25] Assignments of transitions to isolated monomeric species and to molecular complexes are given in Table I. HCl monomer undergoes hindered rotation in Ar; the main perturbation is rotation-translation coupling (RTC).[39-41] Since the crystal potential acts about the center of interaction of the guest, which is displaced from the center of mass for asymmetric molecules, the rotation of the guest is coupled to the oscillation of its center of mass. This center of mass translational motion corresponds to a localized lattice phonon mode.[42,43] RTC produces a complicated pattern of rotational levels and also directly couples the guest

local mode to the IR active guest vibration, producing the $Q_R(00)$ transition (which is a $\Delta v=1$, $\Delta J=0$, $\Delta n=1$ transition, where n is the local mode quantum number).[40] A weaker perturbation is due to the octahedral crystalline field of the Ar lattice which removes the M sublevel degeneracy for all levels with $J \geq 2$.[44] This effect is manifested in the splitting of the R(1) transition of DCl/Ar[45] (Table I). The extreme width of the R(1) transition of HCl/Ar (as seen in Fig. 2) is due primarily to coupling between J=2 and delocalized lattice phonons,[42] but may also reflect unresolved splitting of J=2 by the crystal field. A transition of HCl/Ar at 2914 cm^{-1} has been assigned as R(2) by Barnes.[17] Extension of Friedmann and Kimel's treatment of RTC[41] to include J=3 predicts an R(2) transition at 2917 cm^{-1},[25] in support of Barnes' assignment. An energy level diagram deduced from the HCl/Ar spectra is given in Fig. 3.

Absorption lines due to several non-rotating molecular complexes are included in Table I. Only one strong IR absorption has been assigned to the HCl dimer; several geometries have been proposed for this species.[46,47] The HCl-H_2O complex has not been previously reported in Ar matrices. This very intense absorption is plainly visible even when the H_2O responsible for it cannot be observed at 3757 or 3776 cm^{-1}.[48] The 200 cm^{-1} red shift of the HCl fundamental upon complexation with H_2O is consistent with a 200-300 cm^{-1} red shift observed for HCl upon complexation with H_2O in N_2 matrices.[49] The peak at 2864 cm^{-1} in Ar has been identified[50] as due to an HCl-N_2 complex. The HCl-H_2O and HCl-N_2 peaks are very sensitive

indicators of sample purity; clean samples with neither absorption can be produced.

Absorption spectra of HCl in solid N_2 show no rotational or librational structure.[50] An isotopic doublet at 2854 and 2852 cm^{-1} has been resolved in the present study in samples of M/A = 780 or 1000. The spectrum of HCl/O_2, is qualitatively similar to that of HCl/N_2. An isotopic doublet at 2863 and 2861 cm^{-1} is observed at M/A = 980; no evidence for rotation or libration is found. A plethora of peaks between 2851 and 2736 cm^{-1} grow in subsequent to diffusion.[25]

B. Overtone spectroscopy

Direct measurements of the first overtone absorption required very thick matrices. Matrices of HCl/Ar (M/A = 750), DCl/Ar (M/A = 740) and DCl/N_2 (M/A = 250) were prepared by continuous deposition at 12 K at an average rate of 20 m-mole/hr. For HCl/Ar, R(0), P(1), and R(1) peaks (Table I) are observed in the freshly deposited HCl/Ar sample. Subsequent to diffusion a weak but reproducible peak appears at 5484 cm^{-1}; the latter peak is assigned as dimer. Only one peak, assigned as R(0), was observed in DCl/Ar, and only one peak was observed for DCl/N_2.

Vibrational frequencies and anharmonicities derived from the spectra are given in Table II. Frequencies shift by only 1% from the gas phase and anharmonicities equal gas phase values. The constancy of anharmonicity from gas phase to condensed phase has been observed in other systems.[2,51]

C. Integrated absorption coefficient

From a knowledge of the integrated absorption coefficient of a molecule in a solid it is possible to calculate the molecular transition moment and hence, the radiative lifetime. However, it is difficult to measure the thickness of an optical path through the matrix. Jiang et al.[52] have deduced the absolute absorption coefficient for CO in Ar matrices and pure solid CO by measuring the thickness of their samples by counting interference fringes of a transmitted monochromatic infrared beam during matrix deposition. They found that the ratio of integrated absorption intensity of CO in solid environments to that in the gas phase is accounted for totally by an effective field factor.[52] Likewise, Dubost and Charneau[2] found that the radiative decay rate of vibrationally excited CO in Ar matrices is equal to the gas phase rate corrected for the refractive index of the host.[1] Thus, the transition dipole moment for CO is the same in both the solid environment and the gas phase. Matrices of HCl/CO/Ar were prepared sufficiently dilute (HCl: M/A = 750 - 4360; CO: M/A = 2040, 3940) that multimer absorptions were negligible compared to monomer absorptions. Then integrated absorption coefficient ratios of HCl to CO were measured. No direct measurement of the matrix thickness was required. The samples were prepared and spectra recorded at 9 or 20 K with three different spectral slit widths. A planimeter was used to integrate absorbances for these experiments. The results did not vary with temperature or spectral resolution. The results of five samples gives a value of

0.55 ± 0.05 for the ratio of HCl to CO integrated absorption coefficient. The indicated uncertainty is the standard deviation of a single value from the mean of the five values. This is, within experimental uncertainty, equal to the gas phase ratio of 0.57 ± 0.02.[33,53] Thus, the transition dipole moment of HCl is, like CO, essentially unperturbed by the matrix environment. The radiative lifetime of HCl in solid Ar should be given by the gas phase lifetime multiplied by 0.54 for the local field of the solid.[1] The gas phase radiative lifetimes for HCl v=1 and v=2 are 30.5 and 15 ms;[54] thus, in solid Ar the radiative lifetimes are 16 and 8.1 ms. Gas phase lifetimes for DCl are 95 and 52 ms for v=1 and v=2;[55] thus, its radiative lifetimes in solid Ar are 51 and 28 ms.

Care was taken in the above experiments to exclude the presence of HCl dimer which has an absorption coefficient greater than that of the monomer. The total integrated absorption of an HCl/Ar sample always increased after a diffusion experiment when multimer peaks appeared. In particular, the total integrated absorbance was measured for samples of HCl/Ar of M/A = 980 and 5100 before and after diffusion. The spectra after diffusion consisted of three well-resolved polymeric peaks: dimer, trimer, and high polymer. Assuming the polymeric species have equal transition moments per HCl molecule led to a value of 3 ± 1 for the ratio of the squared transition moment of an HCl molecule in polymeric form to one in monomeric form.

Verstegen et al.[56] measured the absolute absorption coefficient of HCl in solid Ar by counting interference fringes and found the value to be about four times greater in the matrix than in the gas phase. All of their spectra[56] contain significant polymer, which if weighted equally to monomer would increase the absorption coefficient reported. They concluded that the ratio of monomer and polymer absorption coefficients was unity. The cause of the discrepancy between their results and the present results is unclear. Nevertheless, we find the HCl/CO/Ar results compelling evidence that the transition moment of isolated HCl is essentially the same in gas and matrix.

IV. RESULTS

A. Kinetic preliminaries

The OPO excites a single vibration-rotation level of the guest molecule at t=0, and spectrally resolved fluorescence monitors the time evolution of the vibrational excitation. Rapid rotational equilibration following the excitation is assumed. In samples of low concentration where no guest-guest interactions occur, relaxation is due to radiative decay or V→R,P processes (processes 1-3) and population decays are exponential. Subsequent to excitation of N molecules to v=2, the populations of v=2, $n_2(t)$, and v=1, $n_1(t)$, evolve according to

$$n_2(t) = N\, e^{-k_{21}t} \tag{1}$$

$$n_1(t) = \frac{N\, k_{21}}{(k_{21}-k_{10})}\, [e^{-k_{10}t} - e^{-k_{21}t}] \tag{2}$$

where k_{21} and k_{10} are the rates of deactivation of v=2 to v=1 and v=1 to v=0, respectively, and direct deactivation of v=2 to v=0 is neglected. When v=1 is excited initially, $n_1(t)$ decays exponentially with rate k_{10}.

When the guest concentration increases sufficiently, guests may interact with each other by resonantly exchanging vibrational quanta, and energy can migrate about the sample. When a second guest species is present so that energy may be transferred to it, a V→V decay channel opens. Systems in which energy migration and long-range energy transfer by

multipolar interactions compete with V→R,P processes may exhibit time-dependent transfer rates and hence, non-exponential decay kinetics. These rates depend on the relative interaction strengths and concentrations.[1,57] Under conditions for which migration dominates (long times and rapid migration) the V→V transfer rates are time-independent and Eqs. (1) and (2) are valid; individual decay rates have V→R,P and V→V contributions.

All experimental decay curves in this study have been analyzed using Eqs. (1) and (2). There is no clear evidence for long-range energy transfer in the absence of migration. (Decay traces of concentrated samples subsequent to matrix annealing appear to deviate from Eqs. (1) and (2), however.) A more quantitative discussion of migration-assisted energy transfer is presented in Section V-C.

B. HCl/Ar

The HCl/Ar system was the most extensively studied. Decay rates measured by time-resolved fluorescence studies are presented first. Then emission and excitation spectra, which provide additional information on the pathway of relaxation and the identity of relaxing species and finally, unsuccessful attempts to observe fluorescence subsequent to excitation of the dimer are described.

Typical data and analysis for temporally resolved emission following direct excitation of HCl (v=2) in a dilute sample are shown in Figs. 4 and 5. The fluorescence from v=2 decays as a single exponential over at least one and a half decades.

The emission from v=1 rises with the same rate constant with which v=2 decays, and decays with a smaller rate constant. Reciprocal lifetimes, k_{21} and k_{10}, obtained by fitting the data to Eqs. (1) and (2) are presented in Table III for the case of isolated molecules. Decay times for given experimental conditions were measured from spectrally resolved fluorescence and from the total fluorescence. The latter is the sum of two decaying exponentials. Thus each decay rate is measured at least twice. The values listed are either the average of many measurements for equivalent conditions (the uncertainty indicated is the standard deviation of the set of measurements) or only one or two measurements (no uncertainty indicated). In the latter case an uncertainty of 15% is reasonable. In experiments where v=1 was excited directly, values for k_{10} were consistent with those deduced from the v=2 excitation experiments. The observed decay rates are much faster than the radiative decay rates of 120 and 63 sec^{-1} estimated in Section III for HCl v=2 and v=1 in solid Ar. Hence, the radiative decay channel is neglected.

Lifetimes for isolated HCl are insensitive to excitation pulse intensity and frequency. The energy of the excitation pulse was varied by use of neutral density filters. Energy density was varied thirtyfold by using a 4 cm focal length lens to focus excitation into the sample. The degree of focusing was controlled by the position of the lens. While overall S/N was affected by these maneuvers, the temporal behavior of the system was unaffected to within the experimental uncertainty of 10-15%. The spectral width of the OPO (0.2 cm^{-1})

is less than the width of the HCl absorption line (1-2 cm^{-1}) so it was possible to excite various portions of the line profile;decay times were insensitive to this. Furthermore, excitation of any vibration-rotation transition of the isolated monomer, P(1), R(0), R(1), and $Q_R(00)$, results in the same decay kinetics. Excitation on different spots in the matrix gives the same lifetimes.

The decay rate of v=2 is independent of concentration and deposition conditions for M/A = 500-10,000. In a very concentrated sample, M/A = 123, the decay of v=2 fluorescence becomes faster and cannot be fit by a single exponential. It may be analyzed as a double exponential with decay times at 9 K of 60 and 170 μs and an amplitude ratio of 1. The times decrease by factors of 3.5 and 7, respectively, upon increasing the temperature to 21 K. The temperature dependence exhibited by isolated molecules, Table III, is much milder.

The decay rate of v=1 at 9 K is strongly concentration dependent for M/A < 2000, Fig. 6 and Table IV. For M/A < 700, the v=1 decay rate is actually faster than the v=2 decay rate. Equation (2) remains valid in this case, but the rise of v=1 fluorescence corresponds to k_{10} and the peak intensity of the v=1 signal is reduced by the ratio of rate constants in Eq. (2). The rapid decay of v=1 in concentrated samples was verified by measurement of k_{10} following v=1 excitation: in a sample of M/A = 600, $k_{10} = 5.5 \times 10^3$ sec^{-1} at 9 K. For M/A = 123 no v=1 emission was observed, and v=2 decayed non-exponentially at rates in the range 10^4-10^5 sec^{-1}. The absence of v=1

emission shows that $k_{10} > 5 \times 10^5$ sec^{-1}. Decay rates of v=1 at 9 K, 20 K, and the ratio of decay rates at the two temperatures is given for various monomer and dimer concentrations in Table IV. Dimer concentrations were measured relative to monomer by comparing integrated absorption intensities. The monomer concentration was then calculated from the M/A value. The dimer concentrations were calculated assuming that the square of the transition moment per HCl molecule in the dimer is 2.4 times that of the monomer, and is thus subject to a systematic error. Notwithstanding, k_{10} is clearly a strong function of dimer concentration. Deposition conditions affect k_{10} by affecting the dimer concentration.

Both v=2 and v=1 decay rates increase subsequent to annealing. For dilute samples, k_{21} increases by 20-30% (M/A = 1000, 5000). The increase in k_{10} is often a factor of two or more. In concentrated samples, decays sometimes become non-exponential after annealing. Some values of k_{10} subsequent to annealing are included in Table IV. For these samples the decay of v=1 remains exponential.

Fluorescence spectra using the CVF, Fig. 7, show which vibrational levels are populated during the relaxation process. Further, from the relative intensities, the proportion of relaxation by V→V vs V→R,P processes can be estimated. The spectra are insensitive to excitation line and temperature. No emission from any vibrational levels with v>2 is observed. The low frequency tail in the 9 K emission spectrum in Fig. 7 is due to the poor resolution of the CVF (33 cm^{-1}) rather than to any v=3 emission, which must peak at the P(1) line near

2646 cm^{-1}. Emission from v=3 is less than 1% of that from v=2 under focused or unfocused excitation.

The relative fluorescence intensity in Fig. 7 is obtained by integrating the fluorescence decay curve and correcting for radiative lifetime and optical density of the sample:

$$\text{Corrected signal} = (\text{Observed signal})/A\tau\delta \qquad (3)$$

A is the Einstein coefficient and τ is the observed decay time (k_{21}^{-1} for v=2 and k_{10}^{-1} for v=1). The optical density factor, δ, equals one for 2→1 transitions. For the 1→0 band, δ may be calculated for each line from the measured absorption coefficient, using accurate linewidths from the excitation spectra. Due to the nonuniform thickness of the matrix, the absorption experiments sampled shorter average path lengths through the matrix than the fluorescence experiments. Values of δ derived from absorption underestimate the true opacity of the matrix to fluorescence. Nevertheless, a single value of δ, obtained by weighting individual δ's calculated from absorption measurements by a Boltzmann distribution of rotational states in v=1, is used for the entire band.[25] From Eqs. (1)-(3) the ratio of peak heights of 1→0 to 2→1 gives a value ξ, which is the number of molecules produced in v=1 for each molecule excited to v=2. Figure 7 shows values of $0.5<\xi<0.8$. Other methods of estimating δ from the data (based on R(0) intensity, P(1) intensity, or known total amounts of sample deposited) yield $0.5<\xi<1.3$. Thus the experimental data limit ξ only to this range. The simplest mechanism

consistent with these results is sequential V→R,P transfers, v=2 → v=1 followed by v=1 → v=0, which gives ξ=1. Neither V→V(ξ=2) nor two-quantum V→R,P(ξ=0) can be a dominant contributor to the relaxation process. The sequential V→R,P mechanism is further supported by the lack of concentration dependence of k_{21} for M/A>500 (Fig. 6).

No fluorescence was observed upon direct excitation of the overtone of the dimer at 5484 cm^{-1} at 9 or 20 K. In particular, for a sample of M/A = 670, no fluorescence was observed from the dimer at 9 K after averaging 1000 laser pulses. Upon excitation of P(1) under otherwise identical conditions, fluorescence averaged for 4000 pulses produced a 240 μs decay (v=2→1) with S/N = 80. In this sample the fundamental dimer and P(1) absorption intensities were equal at 9 K. In a search for dimer fluorescence, the OPO was moved in 0.7 cm^{-1} increments for 15 cm^{-1} in both directions from 5484 cm^{-1}, and after signal averaging at each setting, no fluorescence was observed. In these experiments, the signal detection bandwidth was 3 MHz. If the ratio of overtone to fundamental absorption is the same for dimer as for monomer, equal absorption intensities of dimer and P(1) mean that the number of molecules excited by the laser pulse is the same for both excitation frequencies. A dimer decay constant of 3 x 10^6 sec^{-1} should have been observable in these experiments.

The fluorescence excitation spectrum in Fig. 8 shows isotopically resolved R(0) and P(1) transitions. Only peaks corresponding to isolated monomeric species are observed in excitation spectra. Searches for emission were made with

several samples following overtone excitation of dimers and other molecular complexes. The range 5720 to 5350 cm^{-1} was scanned at both 9 and 20 K. Signals were observed only for isolated monomeric HCl. Even in a sample with M/A = 123, in which about 10% of the HCl existed in dimeric form, no dimer emission was observed. For the sample of M/A = 670 discussed above, the S/N for the P(1) peak in the excitation spectrum was 35 at 9 K. The intensity of dimer absorption and the lack of dimer fluorescence in this spectrum implies that dimers decay in less than 7 μs. The value of 7 μs as an upper limit for the dimer decay time is consistent with other excitation spectra, and constitutes a conservative bound for the dimer decay time.

In order to see the influence of impurities on the decay rate of isolated HCl, a sample doped with air was prepared (HCl/air/Ar = 1/0.2/930). No new peaks occurred in the fluorescence excitation spectrum of this sample. The presence of massive impurities did not affect the v=2 decay rate at all (see Table III) and the shortening of the v=1 decay rate may be understood in terms of energy transfer to dimer (see Table IV). The amount of air present in this sample is equivalent to the leak rate of the apparatus integrated for 2 x 10^6 hours.

C. DCl/Ar

Some preliminary results on DCl/Ar matrices are included in Table III. Experiments were performed exciting DCl to v=2 on several vibration-rotation transitions and monitoring the spectrally and temporally resolved emission. The DCl experiments

were more difficult than the HCl experiments because both the absorption cross section and the emission intensity are smaller in DCl than in HCl, and the fluorescence signal is proportional to the product of the two. Studies of dilute DCl/Ar samples necessitated rather thick samples, and the fluorescence from v=1 was weakened severely by the optical density on v=1 transitions. Only the k_{21} rate for DCl was reliably determined.

The fluorescence from DCl (v=2) is a single exponential over at least one and a half decades. The decay of v=2, k_{21}, is insensitive to which vibration-rotation transition is excited (P(1), R(0), and both crystal field transitions of R(1)), exact position on the line profile excited, and degree of focusing of the excitation. The relaxation rate of v=2 increases by a factor of 1.7 between 9 and 20 K. Emission from levels other than v=1 or v=2 was sought with the CVF, and none was observed. The value of k_{10} is comparable to k_{21} for the samples in Table III.

Fluorescence excitation spectra of DCl/Ar, as with HCl/Ar, reproduce only monomeric absorption features. In particular, no dimer emission was observed even when excitation spectra were scanned as far red as 3970 cm^{-1}. Considerations such as those presented for the HCl/Ar dimer yield an upper limit for the DCl dimer relaxation time of 160 μs.

The radiative decay rate for DCl (v=2) in Ar was estimated to be 36 sec^{-1}, so as much as 30% of the decay of v=2 may be radiative. The non-radiative decay rate for DCl (v=2) is at least 32 times slower than that for HCl (v-2).

D. HCl/N_2 and HCl/O_2

No fluorescence was observed when HCl was suspended in N_2 or O_2 matrices at M/A = 1000. Direct signal averaging experiments were performed at the v=0→2 absorption frequencies of 5604 and 5621 cm^{-1}, respectively (calculated using gas phase anharmonicities), as well as within a frequency range of 10 cm^{-1} to both sides of these frequencies in 0.7 cm^{-1} increments. If the OPO excited line center of the 0→2 absorption at one of these settings, comparison to the S/N for HCl/Ar systems suggests a lower limit of 6×10^7 sec^{-1} for the relaxation rate.[25] Fluorescence excitation spectra scanned over the ranges 5645-5511 cm^{-1} in N_2 and 5666-5543 cm^{-1} in O_2 yielded no observable peaks. Thus, no species with a lifetime of 10 μs or longer was present.

V. DISCUSSION

The important features of the vibrational relaxation of matrix-isolated HCl and DCl are as follows. In Ar, relaxation is non-radiative (aided slightly by radiation for DCl). For HCl/Ar, k_{21} is independent of concentration and k_{10} is independent of concentration for M/A > 2000. These correspond to isolated molecule V→R,P rates. The relaxation of HCl (v=2) is 32 times faster than that of DCl (v=2), and the relaxation rates increase slightly (less than a factor of 2) over the temperature range 9-20 K. The HCl (v=1) relaxation rate increases as M/A decreases, and at M/A = 123 is too fast to be observable. Molecular complexes, such as dimer, relax very rapidly, as does HCl trapped in molecular solids.

That HCl relaxes more rapidly than DCl is indicative of the role of rotation as the primary energy accepting mode, and will be discussed in Section A. The weak temperature dependence of the isolated molecule relaxation rates may be understood either in terms of phonon participation in the relaxation process or in terms of J-level dependent relaxation, Section B. Migration-assisted V→V transfer to the dimer is suggested as the cause of the concentration dependence of k_{10} in Section C. The dimer, which relaxes rapidly, is a sink for the HCl (v=1) excitation. A value is estimated for the dipole-dipole coupling coefficient between monomer and dimer. The rapid relaxation of the dimer and of HCl in N_2 and O_2 matrices are discussed in Sections D and E.

A. Mechanism of isolated molecule relaxation

Relaxation of a molecular vibration leads to the production of 30 to 40 phonons. Theories of direct multiphonon transfer[58-65] predict that relaxation rates should increase rapidly with temperature and should decrease as the magnitude of vibrational quantum (energy gap) increases. These theories are incompatible with the weak temperature dependence and the violation of the energy gap law for hydride-deuteride systems.

Rotation can be an important accepting mode for hydrides since the change in rotational quantum number for pure V→R transfer is much smaller than the change in phonon number for V→P transfer.[1,7,8] Legay[1] has correlated experimental rate constants with final rotational quantum number for V→R transfer, $J_f = (\nu/cB)^{\frac{1}{2}}$:

$$k \sim \exp(-\alpha J_f). \tag{4}$$

More detailed treatments have appeared.[25,66,67]

For V→R relaxation in Ar of HCl v=2→1, v=1→0, and DCl v=2→1, J_f = 15, 16, and 19 (gas phase B values[28] of 10.5 and 5.45 cm^{-1} for HCl and DCl and matrix vibrational frequencies). The increase in J_f parallels the decrease in relaxation rate for these processes and the data fit nicely into Legay's correlation.[1] The entire relaxation process subsequent to excitation of v=2 of HCl/Ar is shown schematically in Fig. 9. The separation between J=16 and J=15 for HCl is about 340 cm^{-1}. Since it is unlikely that there will be an exact resonance between initial and final vibration-rotation levels in the

relaxing molecule, some participation by phonons (especially local mode phonons) in the V→R step is necessary for energy conservation. Subsequent rotational relaxation in the high J levels will be a multiphonon process, requiring at least five phonons of the Ar lattice in the case of HCl relaxation from J=15 to J=14.

For the V→R step to be rate limiting, R→P transfer must rapidly remove molecules from the rotational levels initially populated by the V→R transfer (Fig. 9). If such were not the case, infrared emission would have been observed from P and R lines near J_f for the 1→0 transition. Furthermore, simple single and double exponential decays would not have been observed. A significant delay in levels near J_f of v=1 would give a v=2 decay rate, k_{21}, faster than the observed rise of emission from the lowest rotational levels of v=1. In addition, significant deviation of the v=1 rotational level distribution from thermal would almost certainly lead to non-exponential decays of v=1.

Level widths of 0.4 and 10 cm^{-1} and corresponding R→P relaxation times of 10 and 0.5 psec have been calculated for J=1 and J=2 of HCl in Ar.[42] Thus, R→P relaxation of higher J levels in times less than 100 μs is not surprising. This rapid transfer among the thermally accessible J levels insures that the observed kinetics must be independent of the J level initially populated by the laser. The observed rates are independent of the rotational line excited and of the precise laser frequency within each line. Homogeneous broadening by R→P transfer could account for the latter observation.

The postulate of rotation as the accepting mode successfully rationalizes the observation that HCl relaxes more rapidly than DCl, but there is no direct evidence that high rotational levels are in fact populated subsequent to vibrational relaxation. This situation is analogous to gas phase vibrational relaxation in which V→R models are successful in correlating a great deal of experimental data, but direct evidence of population of a high rotational level is elusive.[68]

B. Temperature effects

The relaxation rates of HCl/Ar v=2→1 and v=1→0 increase by factors of 1.5 ± 0.2 and 1.3 ± 0.2 between 9 and 21 K. This temperature effect is quite small, but it is real and it is the largest reported temperature effect for V→R,P relaxation of a matrix-isolated species. Vibrational relaxation rates of NH and ND ($A^3\pi$) are independent of temperature to within 10% for T < 25 K in Ar and T < 37 K in Kr,[8] as are those of NH and ND ($X^3\Sigma$) in Ar for T < 30 K.[11] It has recently been observed[10] that the decay time of isolated CH_3F in Kr increases by a factor of about 1.2 between 10 and 60 K. Temperature dependence may result from phonon participation and J dependent relaxation rates.

The V→R step must involve some phonon participation to conserve energy. For exothermic one phonon processes, the relaxation rate will be proportional to $(1 + \bar{n})$, where $\bar{n} = [\exp(hc\nu_p/kT)-1]^{-1}$ is the thermal occupation number of a phonon mode of frequency $c\nu_p$. For endothermic processes rates are proportional to $\bar{n}$ and the temperature dependences predicted

are much greater than experimentally observed. The temperature dependences of k_{21} and k_{10} for HCl/Ar can be fit by exothermic processes requiring one phonon of 12 ± 5 and 20 ± 10 cm^{-1}, respectively, Fig. 10. More than one phonon may be involved in the exothermic process. For higher energy phonons involved (up to 64 cm^{-1} for Ar delocalized phonons[69] and 73 cm^{-1} for the HCl/Ar localized mode) the temperature dependence will be negligible in the range 10-20 K. Temperature dependence is caused only by low frequency phonons created during relaxation.

Relaxation rates probably increase as the initial rotational level of the guest increases. Relaxation rates in the gas phase increase as the velocity of the collision partners increase, and rotational motion effectively adds its tangential velocity to the velocity of the collision pair.[70] The linear translational motion in the solid arises primarily from the local mode oscillation of the guest.[25] At higher temperatures observed relaxation rates should be faster than at lower temperatures, since contributions from excited rotational levels are more heavily weighted. The relaxation rate is:

$$k = \sum_{n,J} f(n,J) k^{n,J} \tag{5}$$

$$f(n,J) = \frac{g_{n,J}}{Q(T)} e^{-E(n,J)/kT}$$

where f(n,J) is the Boltzmann factor for the translation-rotation level (n,J). Q(T) is the guest partition function and $g_{n,J}$, E(n,J), and $k^{n,J}$ are the degeneracy, energy, and relaxation rate of (n,J). (The translational states, n, are included in Eq. (5) in a formal sense only, since the 73 cm^{-1}

energy of n=1 precludes thermal excitation in these experiments.) For HCl/Ar, the partition function can be calculated from the energy level diagram of Fig. 3:

$$Q(T) = 1 + 3e^{-17/kT} + 5e^{-43/kT} + 3e^{-73/kT} + \ldots \qquad (6)$$

with energies expressed in cm^{-1}. If only J=0 and J=1 are considered:

$$k = Q(T)^{-1} k^{0,0} + [1-Q(T)^{-1}]k^{0,1} \qquad (7)$$

From Eq. (6) 89% of the guest HCl is in J=0 or J=1 at 21 K, and even more population resides in these levels at lower temperatures. The data for HCl/Ar are fit to Eq. (7), Fig. 11. The values are: for v=2→1: $k_{21}^{0,0} = (2.9 \pm 0.8) \times 10^3$ and $k_{21}^{0,1} = (7.7 \pm 0.3) \times 10^3\ sec^{-1}$; for v=1→0: $k_{10}^{0,0} = (6.6 \pm 2.3) \times 10^2$ and $k_{10}^{0,1} = (1.4 \pm 0.1) \times 10^3\ sec^{-1}$. The influence of higher levels can be estimated if a form for $k^{n,J}$ is adopted. Assuming that $k^{n,J}$ increases linearly with J, $k^{0,0}$ is unchanged and $k^{0,1}$ is decreased about 20%.

The temperature dependence for HCl/Ar is probably due to a combination of phonon and rotational effects; it is not possible to experimentally distinguish the extent of each. The smaller (null) temperature dependences of the NH and ND relaxation rates may be due to the higher local mode frequencies and larger rotational constants of NH and ND.

C. Energy migration and V→V transfer

The increase of k_{10} for HCl/Ar for M/A < 2000 indicates the appearance of a new deactivation channel. Two effects of increasing concentration may contribute: 1) increased range of V→V transfer to energy accepting species present in the sample; 2) increased concentrations of energy acceptors, such as the HCl dimer. Long-range dipole-dipole coupling provides an explanation for V→V transfer processes between isotopes of CO in Ar[1,2,71] and from NH and ND ($A^2\Sigma$) to various acceptors in Ar.[12]

The mathematical treatment of ensemble kinetics resulting from migration-aided energy transfer by dipolar coupling is problematical. In rigid phases in which donors are randomly distributed, a description of excitation migration in terms of simple diffusion is inappropriate.[72] Hopping models for excitation migration have been developed.[71,73] When energy migration is very rapid, the decay kinetics of non-resonant energy transfer to the acceptor is exponential and independent of the details of migration within the donor system.[1,57,73] In the case where energy migration is not so fast, the donor-acceptor transfer kinetics following pulsed excitation have a non-exponential portion followed by an exponential portion. The mathematical form for the exponential portion of energy transfer in this case depends upon the particular model.[1,57,71,73] Criteria for determining boundaries between regions of different kinetic behavior have been proposed,[73] but are not established. It is argued below that the increase of k_{10} for HCl/Ar in

concentrated samples is due to V→V transfer to the HCl dimer, that this transfer occurs in the limit of rapid excitation migration within the HCl monomer system, and that all transfers involve dipole-dipole interactions.

The rate of energy transfer by coupled dipole-dipole transitions from a donor molecule, D, to an acceptor molecule, A, separated by a distance R is

$$W = C_{DA}/R^6 \tag{8}$$

where C_{DA} is given by Förster-Dexter theory as[74]

$$C_{DA} = \frac{3}{512\pi^6 c n^4 \nu^6} \frac{1}{\tau_D} \frac{1}{\tau_A} \int f_D(\nu)\ f_A(\nu) d\nu \tag{9}$$

where c is the velocity of light in vacuum, n is the refractive index of the host medium, ν is the transition energy expressed in cm^{-1}, τ_D and τ_A are the donor and acceptor radiative lifetimes in vacuum, and $f_D(\nu)$ and $f_A(\nu)$ are the donor and acceptor normalized lineshaped functions expressed in cm^{-1}. For resonant Lorentzian lineshapes of the same FWHM, $\Delta\nu$, the integral is equal to $(\pi\Delta\nu)^{-1}$.

Energy migration results when D=A and can be viewed as a hopping of excitation from one donor to another. Due to the strong distance dependence of the fundamental interaction, Eq. (8), the closest donor molecule to a particular excited donor dominates the energy migration process. Hence, the average hopping rate is given by

$$\langle W \rangle = \int_{R_o}^{\infty} \frac{C_{DD}}{R^6} P(R) dR \tag{10}$$

$$P(R) = 4\pi R^2 \rho x_D \exp(-\frac{4}{3}\pi R^3 \rho x_D) \tag{11}$$

where P(R)dR is the probability that the nearest donor to the excited donor is at a distance between R and R + dR,[71] x_D is the donor mole fraction and ρ is the density of lattice sites (number/cm^3). The lower limit of integration, R_o, reflects the fact that the distribution of HCl monomers is not totally random, since, for example, two HCl molecules in adjacent sites comprise a dimer and do not participate in energy migration. The distribution of HCl monomer is assumed to be random for separations greater than R_o. All smaller separations are eliminated by aggregation (most likely to dimer) during deposition. (When R_o is larger than one nearest neighbor separation, the difference between an integral, Eq. (10), and a more precise lattice sum is at most a few percent.) The result of integration gives

$$\langle W \rangle = \frac{4\pi\rho x_D C_{DD}}{3R_o^3}[1-1.77\rho x_D R_o^3 + \ldots]. \tag{12}$$

For cases considered subsequently, the second term is less than 10% of the first and can be neglected.

Calculation of <W> requires values for R_o and C_{DD}. A value for R_o may be estimated. Given an HCl molecule at the origin, the random probability of another being within R_o of the first is $\frac{4}{3}\pi R_o^3 \rho x_{HCl}$, where x_{HCl} is the reciproval M/A value, and the probability is much less than one. The ratio of monomers to dimers is just half this probability:

$$\frac{x_{dimer}}{x_{monomer}} = \frac{2}{3}\pi R_o^{\,3}\rho x_{HCl} \tag{13}$$

Values of R_o are calculated from the measured monomer and dimer concentrations of Table IV. R_o is in the range of 4-6 Å, for the unannealed samples, which corresponds to a physically reasonable distance of almost two nearest neighbor separations. An annealing operation permits limited solute diffusion. The increases in R_o to 13 and 19 Å shown in Table IV demonstrate sensitivity to the precise temperature-time profile.

For C_{DD}, the integral of Eq. (9) becomes a Boltzmann-weighted sum of integrals for coupled transitions. The relevant transitions for HCl/Ar are R(0), P(1), R(1), and P(2). Assuming Lorentzian lineshapes, the integral is

$$\int \frac{f_D(\nu)\, f_A(\nu)\, d\nu}{\nu^6} = \sum \frac{1}{\nu_{ij}^{\;6}} \frac{1}{\pi\Delta\nu_{ij}}\, f(n_i,J_i)\; f(n_j,J_j) \tag{14}$$

where ν_{ij} and $\Delta\nu_{ij}$ are the frequency (cm^{-1}) and linewidth of the transition connecting rotation-translation level (n_i,J_i) of v=1 with (n_j,J_j) of v=0.

The average number of resonant hops made during the V→R,P lifetime τ of the excitation, $\mathcal{N} = \langle W\rangle\, \tau$, is calculated from Eqs. (9), (12), and (14), using Boltzmann factors from Eq. (6) and an average R_o = 5 Å. The results for v=1 and v=2 excitation are given in Table V for several M/A ratios. Linewidths used are 1.3 (9 K) and 2.4 (20 K) for R(0) and P(1) lines and 9 cm^{-1} for R(1) and P(2) lines.

Most of the resonant transfer occurs via P(1) and R(0) transitions. The width of the level J=2 and its small thermal populations make the terms in Eq. (14) corresponding to R(1) and P(2) contribute less than 0.1% an 9 K and less than 6% at 20 K to the resonant transfer rate. That relaxation of v=2 should be concentration independent is immediately obvious upon examination of Table V, since for M/A > 500 v=2 excitation makes less than one hop during its V→R,P lifetime. The immobility of v=2 excitation is due to the small overtone transition moment, and hence a small C_{DD}.

It is apparent from Table V that v=1 excitation moves substantially during its V→R,P lifetime; even in the most dilute sample of M/A = 10,000 v=1 excitation makes a thousand hops. At M/A = 1000, v=1 excitation makes 16,000 hops. How much motion of the v=1 vibron is enough to be considered fast migration? The salient physical feature of the fast migration regime is that the excitation inhabits enough donor sites during its lifetime so that the entire range of D-A interactions is statistically sampled by all vibrons. As a criterion for the fast migration regime, it is required that the vibron hop to at least one site with a nearby acceptor, so that the strongest and least probable D-A interaction is sampled. If the nearby acceptor were in the nearest neighbor shell, the HCl molecule would not be isolated, so nearby will be taken as the sphere of neighbors just beyond the first nearest neighbor shell (another choice might be the shell of neighbors at R_o).

For fcc lattices there are 42 sites between one and two nearest neighbor distances.[75] The condition for fast migration is

$$42\,\eta x_A > 1 \tag{15}$$

where x_A is the acceptor mole fraction. For M/A = 1000 at 9 K, the data of Table V suggest that for $x_A > 2 \times 10^{-6}$, V→V transfer is in the fast migration regime.

The likely acceptor for v=1 excitation is the HCl dimer, since its infrared active vibrational level at 2818 cm^{-1} is more nearly resonant with HCl monomer than with other polymeric species, and non-resonant V→V probabilities decrease as the energy gap between donor and acceptor increases.[12] Indeed, transfer of excitation by a coupled P(1) transition of the monomer with excitation of the dimer is exothermic by 36 cm^{-1}, which corresponds to a peak in the phonon spectrum of Ar,[69] resulting in a large density of final states for this process. Using dimer concentrations from Table IV, Eq. (15) is satisfied by a factor of 5-10 at M/A = 1000, and for this and more concentrated samples V→V transfer to dimer is described in the fast migration regime.

In the fast migration regime, all donor sites are equivalent and the time-independent transfer rate is given by[1,73]

$$k_{10} = k_o + C_{DA} x_A \sum_i \frac{1}{L_i^{\,6}} \tag{16}$$

where k_o is the unimolecular V→R,P rate and the sum is over all lattice points, at distances L_i from the origin. Assuming that monomers and dimers have a minimum separation of R_o, the sum in

Eq. (16) is evaluated as an integral to give

$$k_{10} = k_o + \frac{4\pi\rho x_A C_{DA}}{3R_o^3}. \tag{17}$$

Values for C_{DA} for monomer-dimer coupling are calculated from Eq. (17) and presented for 9 and 20 K data in Table IV. Values are calculated only for those samples for which the uncertainty in $(k_{10}-k_o)$ is less than the magnitude. The average for C_{DA} is performed on logarithms of C_{DA}, and the error is one standard deviation of the fit.

The average C_{DA} at 9 K, 4×10^{-38} cm^6/sec (range is 2.0 to 8.0×10^{-38}) should be compared to the monomer C_{DD} value for R(0) or P(1) transitions, which is calculated to be 4.6 $\times 10^{-35}$ cm^6/sec. The value of C_{DA} depends somewhat on the choice of R_o. If monomer-dimer pairs are allowed to occupy all relative positions except nearest neighbor, the C_{DD} values obtained from Eq. (16) are 50% larger than those in Table IV. The dimer concentrations have an uncertainty of up to a factor of 2 due to the value chosen for the dimer transition moment, and this uncertainty is passed on to C_{DA}. In view of the range of individual C_{DA} values, these uncertainties are not important. Certainly $C_{DA} = 10^{-37.4\pm1}$ cm^6/sec is safe.

It is conceivable that migration aids V→V transfer to an unidentified trace contaminant in the system. In particular, the HCl-N_2 complex absorption is nearly resonant with HCl monomer. However, the HCl-N_2 complex could be reduced to subspectroscopic concentration and was for most samples. The C_{DA} value for V→V transfer to the dimer obtained from the

air-doped sample (Table IV) is consistent with values of other samples, so the substantial impurities present in this sample do not accept a large fraction of the excitation. The effect of systematic impurities in either the HCl or Ar reagents used cannot explain the data of Table IV.[25] The large concentration and near-resonance of the dimer make it the best candidate for energy acceptor. It is possible, however, that uncontrolled and often unknown (subspectroscopic) concentrations of HCl-N_2 could be responsible for some scatter in the V→V data.

In summary, the increase of k_{10} with decreasing M/A has been interpreted as migration-aided, dipole-dipole V→V transfer to the HCl dimer. The migration is rapid enough to average all monomer sites with respect to dimers, and a value of the monomer-dimer coupling coefficient, C_{DA}, has been deduced. Monomer-dimer coupling is 1000 times weaker than monomer-monomer coupling.

D. Dimer relaxation

No fluorescence is observed upon excitation of the HCl dimer at 9 or 20 K, implying that the relaxation of the IR active dimer vibration is probably faster than 0.3 μs and certainly faster than 7 μs. Energy is most probably transferred to the bending modes of the dimer. The higher frequency modes of polyatomics are known to relax rapidly by way of lower frequency vibrations.[76] Thus it is not surprising that the HCl dimer is a sink for vibrational energy. The second stretching vibration is unlikely to play a role if it is

higher in energy than the strongly IR active vibration.[47] If it is lower in energy, relaxation could proceed through the second stretching vibration. If the two levels are separated by less than 30 cm^{-1},[77] then the second vibration cannot be a bottleneck in order for no dimer emission to be observed at 20 K.

E. Relaxation in N_2 and O_2 matrices

Spectroscopic observations indicate that at thermal energies below 20 K HCl does not undergo rotation in the molecular matrices N_2 and O_2. It is unlikely that the barrier to rotation is as large as 2800 cm^{-1}, however, so at energies corresponding to that of a vibrational quantum, rotational motion should be less restricted. Vibrational relaxation into rotational motion should occur on a time scale similar to that for HCl/Ar. V→V transfer from HCl to the vibron band of the host lattice is a possibility in N_2 and O_2 host lattices that is not present in an Ar lattice, and it is likely that the lack of observable fluorescence from HCl in the molecular lattices is due to such rapid V→V transfer. Transfer from HCl to the vibron band of α-N_2 at 2327 cm^{-1} [78] is exothermic by about 500 cm^{-1} and would be a low order and hence, rapid process if excess energy is absorbed by local modes or lattice phonons. Once the excitation has entered the host vibron band it cannot be observed in fluorescence, although it may persist for times as long as one second.[4] It is somewhat surprising that V→V transfer to the α-O_2 vibron mode at 1552 cm^{-1} [79] is

so fast that no HCl fluorescence is observed, since 1200 cm^{-1} must be dissipated into phonons, local modes or rotational motion. However, α-O_2 has higher frequency acoustic modes than Ar.[79]

VI. SUMMARY AND CONCLUSIONS

In this work relaxation rates have been measured for v=2 and v=1 of HCl/Ar as a function of concentration and temperature, and for v=2 in dilute samples of DCl/Ar as a function of temperature. The non-radiative relaxation rate for v=2 of HCl/Ar is 32-45 times faster than for v=2 of DCl/Ar, in spite of the fact that HCl has a larger vibrational frequency than DCl, and so must ultimately transfer more energy to the host lattice. The rates increase only slightly (less than two-fold) between 9 and 21 K. These results indicate that V→R relaxation occurs. The rate limiting step is creation of a highly rotationally excited guest molecule. Subsequent relaxation of rotation into lattice phonons is rapid. The weak temperature dependence is due to low-order phonon participation and/or variation of relaxation rate with particular quantum level of the excited guest.

Relaxation of HCl/Ar (v=2) is independent of concentration for M/A > 500. The relaxation rate from v=1 is concentration independent for M/A > 2000, and rises rapidly for M/A < 1000. The increase is due to energy migration of v=1 excitation from monomer to monomer by resonant dipole-dipole coupling which allows energy to be irreversibly transferred to the HCl dimer. Direct excitation experiments indicate that the dimer relaxes very rapidly and hence dimer, which is present in increasing concentration as M/A decreases, acts as an energy sink. The relaxation of v=2 is much less sensitive to dimer (and all other guest species) since resonant transfer of two quanta is

too weak to produce energy migration. It has been argued that for HCl/Ar migration-assisted V→V transfer to the dimer belongs to the fast migration regime, and the monomer-dimer coupling coefficient has been estimated on this basis. In N_2 and O_2 matrices, HCl relaxation is too rapid for observation, presumably due to V→V transfer to the host.

Spectroscopic experiments show that the transition moment of HCl monomer in Ar is not perturbed noticeably by the matrix environment. Also, the anharmonicity of HCl and DCl in Ar and N_2 matrices is unchanged from gas to matrix.

VII. ACKNOWLEDGEMENTS

We are grateful to the U. S. Army Research Office, to the National Science Foundation and to the Division of Nuclear Research and Applications of the Department of Energy for research support. JMW appreciates fellowship support from the National Science Foundation and the IBM Corporation's University of California-University Fellowship. We thank Lester Andrews for use of his matrix isolation apparatus at Berkeley, on which some of the overtone absorption spectra were taken. We are grateful to H. Dubost and F. Legay for communication of their results prior to publication, and to Linda Young for suggestions on the manuscript.

REFERENCES

1. F. Legay, in Chemical and Biochemical Applications of Lasers, Vol. II, C.B. Moore, ed., Academic Press, New York (1977), Chapter 2.
2. H. Dubost and R. Charneau, Chem. Phys., 12, 407 (1976).
3. L. J. Allamandola, H. M. Rojhantalab, J. W. Nibler, and T. Chappell, J. Chem. Phys., 67, 99 (1977).
4. K. Dressler, O. Oehler, and D. A. Smith, Phys. Rev. Lett., 34, 1364 (1975).
5. D. S. Tinti and G. W. Robinson, J. Chem. Phys., 49, 3229 (1968).
6. S. R. J. Brueck and R. M. Osgood, Chem. Phys. Lett., 39, 568 (1976).
7. L. E. Brus and V. E. Bondybey, J. Chem. Phys., 63, 786 (1975).
8. V. E. Bondybey and L. E. Brus, J. Chem. Phys., 63, 794 (1975).
9. L. Abouaf-Marguin, H. Dubost, and F. Legay, Chem. Phys. Lett., 22, 603 (1973).
10. L. Abouaf-Marguin, B. Gauthier-Roy, and F. Legay, Chem. Phys., 23, 443 (1977).
11. V. E. Bondybey, J. Chem. Phys., 65, 5138 (1976).
12. J. Goodman and L. E. Brus, J. Chem. Phys., 65, 1156 (1976).
13. J. D. Baldeschwieler and G. C. Pimentel, J. Chem. Phys. 33, 1008 (1960) and R. T. Hall and G. C. Pimentel, J. Chem. Phys., 38, 1889 (1963).

14. R. V. Ambartzumian, Yu. A. Gorokhov, G. N. Makarov, A. A. Puretzky, and N. P. Furzikov, in Laser Spectroscopy III, J. L. Hall and J. L. Carlsten, eds., Springer-Verlag, Berlin (1977).

15. B. Davies, A. McNeish, M. Poliakoff, and J. J. Turner, J. Am. Chem. Soc., 99, 7573 (1977).

16. H. E. Hallam, in Vibrational Spectroscopy of Trapped Species, H. E. Hallam, ed., Wiley, New York (1973), Chapter 3.

17. A. J. Barnes, in Vibrational Spectroscopy of Trapped Species, H. E. Hallam, ed., Wiley, New York (1973), Chapter 4.

18. J. M. Farrar and Y. T. Lee, Chem. Phys. Lett., 26, 428 (1974).

19. S. E. Novick, P. Davies, S. J. Harris, and W. Klemperer, J. Chem. Phys., 59, 2273 (1973).

20. S. E. Novick, K. C. Janda, S. L. Holmgren, M. Waldman, and W. Klemperer, J. Chem. Phys., 65, 1114 (1976).

21. A. W. Miziolek and G. C. Pimentel, J. Chem. Phys. 65, 4462 (1976).

22. W. B. Neilsen and R. G. Gordon, J. Chem. Phys., 58, 4149 (1973).

23. R. V. Steele and C. B. Moore, J. Chem. Phys. 60, 2794 (1974).

24. V. E. Bondybey, J. Chem. Phys., 66, 995 (1977).

25. J. M. Wiesenfeld, Ph.D. Thesis, University of California, Berkeley (1977).

26. R. N. Perutz and J. J. Turner, J. Chem. Soc. Faraday Trans. II, 69, 452 (1973).

27. L. J. Allamandola, Ph.D. Thesis, University of California, Berkeley (1973).

28. D. H. Rank, D. P. Eastman, B. S. Rao, and T. A. Wiggins, J. Opt. Soc. Am., 52, 1 (1962).

29. S. R. Leone and C. B. Moore, Chem. Phys. Lett., 19, 340 (1973).

30. A. Hordvik and P. B. Sackett, Applied Optics, 13, 1060 (1974).

31. J. Wormhoudt, J. I. Steinfeld, and I. Oppenheim, J. Chem. Phys., 66, 3121 (1977).

32. The v=0→v=2 absorption cross-section for gaseous HCl is 36 times smaller than the fundamental absorption (Ref. 33).

33. R. A. Toth, R. H. Hunt and E. K. Plyler, J. Mol. Spect., 35, 110 (1970).

34. The thermal decay time is found by solving a diffusion equation in cylindrical coordinates. It is multi-exponential with the slowest exponential having the decay time $\tau = \rho c r_o^2/5.784k$ where ρ = density of the solid, c = specific heat, r_o = radius of heated volume, and k = thermal conductivity (Ref. 35). The following values for solid Ar at 10 K are used (Ref. 36): $\rho = 1.8$ g/cm^3; c = 0.083 J/g-K; k = 35 mW/cm-K. For $r_o = 30$ μ, $\tau = 6.6$ μs.

35. H. S. Carslaw and J. C. Jaeger, Conduction of Heat in Solids, Second Edition, Clarendon Press, Oxford (1959), p. 199.

36. E. R. Dobbs and G. O. Jones, Rept. Prog. Phys., 20, 516 (1957).

37. The CVF used in these experiments (Optical Coating Laboratories, Inc.) has a range of 3 to 6 μ.

38. The gating circuit is described by H. Rosen, P. Robrish, and G. Jan de Vries, Rev. Sci. Instrum., 46, 1115 (1975).

39. H. Friedmann and S. Kimel, J. Chem. Phys., 43, 3925 (1965).

40. H. Friedmann and S. Kimel, J. Chem. Phys., 44, 4359 (1966).

41. H. Friedmann and S. Kimel, J. Chem. Phys., 47, 3589 (1967).

42. P. D. Mannheim and H. Friedmann, Phys. Stat. Sol., 39, 409 (1970).

43. A. S. Barker and A. J. Sievers, Rev. Mod. Phys., 47, Suppl. 2 (1975).

44. A. F. Devonshire, Proc. Royal Soc. (London), A153, 601 (1936).

45. J. B. Davies and H. E. Hallam, Trans. Faraday Soc., 67, 3176 (1971).

46. B. Katz, A. Ron, and O. Schnepp, J. Chem. Phys., 47, 5303 (1967).

47. L. C. Brunel, J. C. Bureau and M. Peyron, Chem. Phys. 28, 387 (1978).

48. R. L. Redington and D. E. Milligan, J. Chem. Phys., 37, 2162 (1962).

49. B. S. Ault and G. C. Pimentel, J. Phys. Chem., 77, 57 (1973).

50. M. T. Bowers and W. H. Flygare, J. Chem. Phys., 44, 1389 (1966) and D. E. Mann, N. Acquista, and D. White, J. Chem. Phys., 44, 3453 (1966).

51. S. R. J. Brueck, T. F. Deutsch, and R. M. Osgood, Chem. Phys. Lett., 51, 339 (1977).

52. G. J. Jiang, W. B. Person, and K. G. Brown, J. Chem. Phys., 62, 1201 (1975).

53. R. A. Toth, R. H. Hunt, and E. K. Plyler, J. Mol. Spect., 32, 85 (1969).

54. J. K. Cashion and J. C. Polanyi, Proc. Royal Soc. (London), A258, 529 (1960).

55. F. G. Smith, J. Quant. Spect. Rad. Transfer, 13, 717 (1973).

56. J. M. P. J. Verstegen, H. Goldring, S. Kimel, and B. Katz, J. Chem. Phys., 44, 3216 (1966).

57. M. J. Weber, Phys. Rev., B4, 2932 (1971).

58. A. Nitzan and J. Jortner, Mol. Phys., 25, 713 (1973).

59. A. Nitzan, S. Mukamel, and J. Jortner, J. Chem. Phys., 60, 3929 (1974).

60. A. Nitzan, S. Mukamel, and J. Jortner, J. Chem. Phys., 63, 200 (1975).

61. J. Jortner, Mol. Phys., 32, 379 (1976).

62. D. J. Diestler, J. Chem. Phys., 60, 2692 (1974).

63. S. H. Lin, J. Chem. Phys., 61, 3810 (1974).

64. S. H. Lin, H. P. Lin, and D. Knittel, J. Chem. Phys., 64, 441 (1976).

65. S. H. Lin, J. Chem. Phys., 65, 1053 (1976).

66. K. F. Freed and H. Metiu, Chem. Phys. Lett., 48, 262 (1977).

67. R. B. Gerber and M. Berkowitz, Phys. Rev. Lett., 39, 1000 (1977).

68. See however, G. D. Downey, D. W. Robinson, and J. H. Smith, J. Chem. Phys., 66, 1685 (1977).

69. D. N. Batchelder, M. F. Collins, B. C. G. Haywood, and G. R. Sidey, J. Phys. C, Sol. State Phys., 3, 249 (1970).

70. C. B. Moore, J. Chem. Phys., 43, 2979 (1965).

71. A. Blumen, J. Manz, and V. Yakhot, Chem. Phys., 26, 287 (1977).

72. S. W. Haan and R. Zwanzig, J. Chem. Phys., 68, 1879 (1978).

73. Yu. K. Voron'ko, T. G. Mamedov, V. V. Osiko, A. M. Prokhorov, V. P. Sakun, and I. A. Shcherbakov, Sov. Phys. JETP, 44, 251 (1976).

74. From Ref. 1, except that n is raised to the fourth power.

75. J. O. Hirschfelder, C. F. Curtiss, and R. B. Bird, Molecular Theory of Gases and Liquids, Wiley, New York (1954), p. 1037.

76. K. Spanner, A. Laubereau, and W. Kaiser, Chem. Phys. Lett., 44, 88 (1976).

77. A. J. Barnes, H. E. Hallam, and G. F. Scrimshaw, Trans. Faraday Soc., 65, 3150 (1969).

78. A. Anderson, T. S. Sun, and M. C. A. Donkersloot, Can. J. Phys., 48, 2265 (1970).

79. J. E. Cahill and G. E. Leroi, J. Chem. Phys., 51, 97 (1969).

Table I. Absorption frequencies of HCl and DCl in some matrices[a]

	Assignment	HCl frequency	DCl frequency
Ar Matrix:	$Q_R(00)$	2944	2149
	R(2)	2913	2108
	R(1) $T_{1u}\rightarrow E_g$	2897	2099[c]
	R(1) $T_{1u}\rightarrow T_{2g}$		2095[c]
	R(0) $H^{35}Cl$	2888	2090
	R(0) $H^{37}Cl$	2886	2088
	P(1) $H^{35}Cl$	2854	2070
	P(1) $H^{37}Cl$	2852	2067
	P(2)	2844	2061
	$HCl-N_2$[b]	2864	2073
	$HCl-H_2O$[c]	2665	1935
	dimer	2818	2040
	timer	2786	2019
	R(1)[d]	5663	
	R(0)[d]	5656	4117
	P(1)[d]	5622	
	dimer[d]	5484±2	
N_2 matrix:[c]	^{35}Cl monomer	2855	2067
	^{37}Cl monomer	2853	2065
	Monomer[d]		4080
O_2 matrix:[c]	^{35}Cl monomer	2863	
	^{37}Cl monomer	2861	

[a]Unless otherwise specified, frequencies and assignments are from Hallam, Ref. 16. All frequencies are accurate to ±1 cm^{-1} unless other error limits are quoted.

[b]From Ref. 50.

[c]This work.

[d]Overtone absorptions from this work.

Table II. Frequency and anharmonicity for HCl and DCl in various matrices (cm^{-1})

System[a]	$\omega_{0\to1}$[b]	$\omega_{0\to2}$[b]	ω_e	$\omega_e x_e$
HCl(gas)[c]	2886	5668	2991	52
HCl/Ar	2871 ± 1	5639 ± 1	2974 ± 4	52 ± 2
HCl/N_2	2855 ± 1			
HCl/O_2	2863 ± 1			
$(HCl)_2/Ar$	2818 ± 1	5484 ± 2	2970 ± 5	76 ± 2
DCl(gas)[c]	2091	4128	2145	27
DCl/Ar	2080 ± 1	4107 ± 1	2133 ± 4	27 ± 2
DCl/N_2	2067 ± 1	4080 ± 1	2121 ± 4	27 ± 2

[a] Values used are for the ^{35}Cl isotope.

[b] Pure vibrational frequency is $[\omega_{R(0)} + \omega_{P(1)}]/2$.

[c] From Ref. 28. Uncertainties are less than 10^{-3} cm^{-1}.

Table III. Relaxation rates for isolated molecules in Ar (10^3 sec^{-1})

M/A	T(K ± 0.4)									
	9.1	12	14	15	16	17	18	19	20	21
HCl: v=2→1										
527±5	3.59±0.07									5.6
670±20	3.7±0.3								5.5±0.2	
930±30[a]	3.6±0.5				4.2				4.9	
960±20	4.2±0.6					5.7±0.7			6.3±0.2	
980±30	3.8±0.6	4.7		4.6			4.9		5.8	
2900±30	4.7±1.2[b]		4.7±1.0		5.6			5.1±0.5		6.2±1.6
5100±100	3.7±0.2	4.5±0.6		5.3±0.8			5.6±0.5			6.0
10,000±1000	3.7±0.2	4.5±0.2	4.6±0.2			4.9±0.3			5.4±0.8	
Average	3.8±0.4	4.6±0.5							5.7±0.6	
HCl: v=1→0										
2380±60[c]	0.88±0.09	0.82		0.96		1.0[d]				1.2
2900±30	0.84±0.09		0.89		1.0			1.1±0.1		1.1±0.1
5100±100	0.76±0.09	0.85±0.10		0.82±0.05			0.89			0.93
10,000±1000	0.75±0.02	0.77	0.98						1.0	
Average	0.81±0.07	0.81±0.04								1.1±0.1
DCl: v=2→1										
3270±60	0.11±0.01	0.13		0.17						
4800±100	0.12±0.01	0.15		0.18			0.19		0.20±0.01	
Average	0.12±0.02	0.14±0.02		0.18±0.01						

[a] Air-doped sample: HCl/Air/Ar = 1/0.2/930.

[b] Value discarded in computing averages.

[c] Direct v=1 excitation.

[d] 17.5 K.

Table IV. HCl v=1→0 Relaxation data and monomer-dimer coupling coefficients

M/A	Mole fractions (10^{-3})		k_{10} ($10^3 sec^{-1}$)		$\frac{k(20)}{k(9)}$	R_o[a] (Å)	C_{DA} ($10^{-37} cm^6/sec$)[b]	
	$x_{monomer}$	x_{dimer}	9 K	20 K[c]			9 K	20 K
123±2	6.6 ±0.1	0.68 ±0.01	>500	>500		4.0		
527±5	1.78 ±0.02	0.049±0.005	8.5 ±2.5	27±7	3.1±1.7[g]	4.0	0.94	3.1
600±30[d]	1.58 ±0.08	0.028±0.002	5.5 ±0.3			3.7	0.78	
670±20	1.46 ±0.06	0.030±0.005	6.5 ±1.8	11±3	1.7±0.9	4.0	1.1	2.0
920±30[d]	1.00 ±0.03	0.033±0.003	0.95±0.11	1.1	1.2	5.2		
920±30[e]	0.50 ±0.02	0.14 ±0.02	1.9			13	1.6	
930±30[f]	1.00 ±0.03	0.026±0.003	1.6 ±0.2	2.0	1.3	4.8	0.31	0.39
960±20	1.03 ±0.03	0.017±0.005	1.2 ±0.2	1.5	1.3	4.1	0.15	0.19
980±30	1.00 ±0.03	0.020±0.003	1.2 ±0.1			4.4	0.16	
990±20	0.91 ±0.03	0.016±0.002	1.6 ±0.3	2.1±0.3	1.3±0.4	4.4	0.39	0.54
1000±20	0.89 ±0.02	0.038±0.004	2.0 ±0.2	2.2±0.6	1.1±0.4	5.9	0.60	0.60
2380±60[d]	0.38 ±0.01	0.004±0.001	0.88±0.09	1.2	1.4	5.0		
2900±30	0.345±0.003	<0.004	0.84±0.09	1.1	1.3	<5.3		
5100±100	0.196±0.004	<0.004	0.76±0.09	0.93	1.2	<7.7		
5100±100[e]	0.118±0.006	0.026±0.002	0.88±0.06			19		
10,000±1000	0.10 ±0.01	<0.004	0.76±0.02	1.0	1.3	<12		
Average[h]					1.3±0.2	4.5±0.7[i]	$10^{-37.4\pm0.3}$	$10^{-37.1\pm0.5}$

Footnotes for Table IV

[a] Calculated from Eq. (13).

[b] Calculated from Eq. (17).

[c] T = 20 ± 1 K.

[d] Direct excitation of v=1.

[e] Sample prepared by annealing sample listed directly above it in the table.

[f] Air-doped sample: HCl/Air/Ar = 1/0.2/930.

[g] This value discarded in averaging k(20)/k(9).

[h] Error is one standard deviation of the data set.

[i] Annealed samples are not included in the average.

Table V. Resonant hops for v=1 and v=2 of HCl/Ar[a,b]

M/A	v = 0 ↔ v = 1		v = 0 ↔ v = 2	
	η(9 K)	η(20 K)	η(9 K)	η(20 K)
100	1.6(5)	7.8(4)	4.1	1.7
500	3.1(4)	1.6(4)	.82	.35
1,000	1.6(4)	7.8(3)	.41	.17
2,500	6.2(3)	3.1(3)	.16	.069
5,000	3.1(3)	1.6(3)	.082	.035
10,000	1.6(3)	7.8(2)	.041	.017

[a] Powers of ten in parentheses: 1.6(5) = 1.6×10^5.

[b] Lifetimes used are τ(v=1, 9 K) = 1.3 ms, τ(v=1, 20 K) = 1.0 ms, τ(v=2, 9 K) = 0.28 ms and τ(v=2, 20 K) = 0.18 ms.

FIGURE CAPTIONS

Fig. 1. Schematic for fluorescence experiments. The output of the OPO is collimated, filtered, and directed into the matrix; sometimes the excitation is focused, as shown. Fluorescence is focused onto a cooled Ge:Hg photoconductive detector. A photodiode pulse, synchronized with the Nd:YAG pulse, triggers the electronics.

Fig. 2. Representative absorption spectrum of HCl/Ar. Deposition conditions: 9 K, 6 mmoles/hr; total deposited = 15 mmoles.

Fig. 3. Energy level diagram for HCl/Ar. The spacings are derived from the data of Table I, and the finite widths of the levels are neglected. J is the rotational quantum number and n is the local phonon mode (translational) quantum number.

Fig. 4. Spectrally resolved decay traces from HCl/Ar, M/A = 5100 ± 100, 18.2 ± 0.2 K. Excitation is at 5656 cm^{-1}, v=0→2, $R(0)^{35}$ transition, with 8 μJ/pulse energy. Curve a is v=2→1 fluorescence and is the averaged signal of 2048 shots. Curve b is the v=0→1 fluorescence and is the averaged result of 4096 shots. The reduced S/N of curve b as compared to curve a is due to poor overlap of the spectrally resolving interference filter and the v=1→0 emission band. The baseline undershoot of curve b is the result of 60 Hz pickup. Deposition conditions: 9 K, 23 mmoles/hr; total deposited = 52 mmoles.

Fig. 5. Analysis of spectrally resolved decay traces of Fig. 4. Curve a (●) is a single exponential, Eq. (1), and curve b (O,□) is the sum of a rising and falling exponential, Eq. (2).

Fig. 6. Concentration dependence of HCl/Ar relaxation rates at 9 K. Samples shown were deposited under similar conditions: 9 K and 20-30 mmole/hr. Data is from Tables III and IV.

Fig. 7. Fluorescence spectra of HCl/Ar, M/A = 1000 ± 20. The histograms are normalized line emission spectra calculated for a Boltzmann distribution of rotational levels of the emitting vibrational level; P and R lines are indicated for v=3→2, v=2→1, and v=1→0 bands. Lowest trace is data uncorrected for optical density of v=1→0 transitions.

Fig. 8. Fluorescence excitation spectrum for overtone excitation, HCl/Ar, M/A = 980 ± 30, 9 K. Deposition conditions: 9 K, 19 mmoles/hr; total deposited = 12 mmoles.

Fig. 9. Overall schematic of relaxation of HCl(v=2)/Ar. The rate limiting steps are V→R processes, k_{21} and k_{10}. The V→R step produces a highly excited rotational level which can rapidly relax by energy transfer to phonons, n. The phonons shown are 73 cm^{-1} energy, corresponding to the HCl/Ar local mode.

Fig. 10. Temperature dependence attributed to phonon participation in HCl/Ar V→R processes. Data are isolated molecule V→R,P rates from Table III. The solid curves are calculated for exothermic phonon processes and are normalized to the 9 K relaxation rate; the phonon energies are indicated in cm^{-1}.

Fig. 11. Temperature dependence attributed to variation of rate with J-level. Isolated molecule V→R rates of Table III are fit to Eq. (7); $n_0(T) = Q(T)^{-1}$ is the fraction of molecules in J=0. Results are in the text.

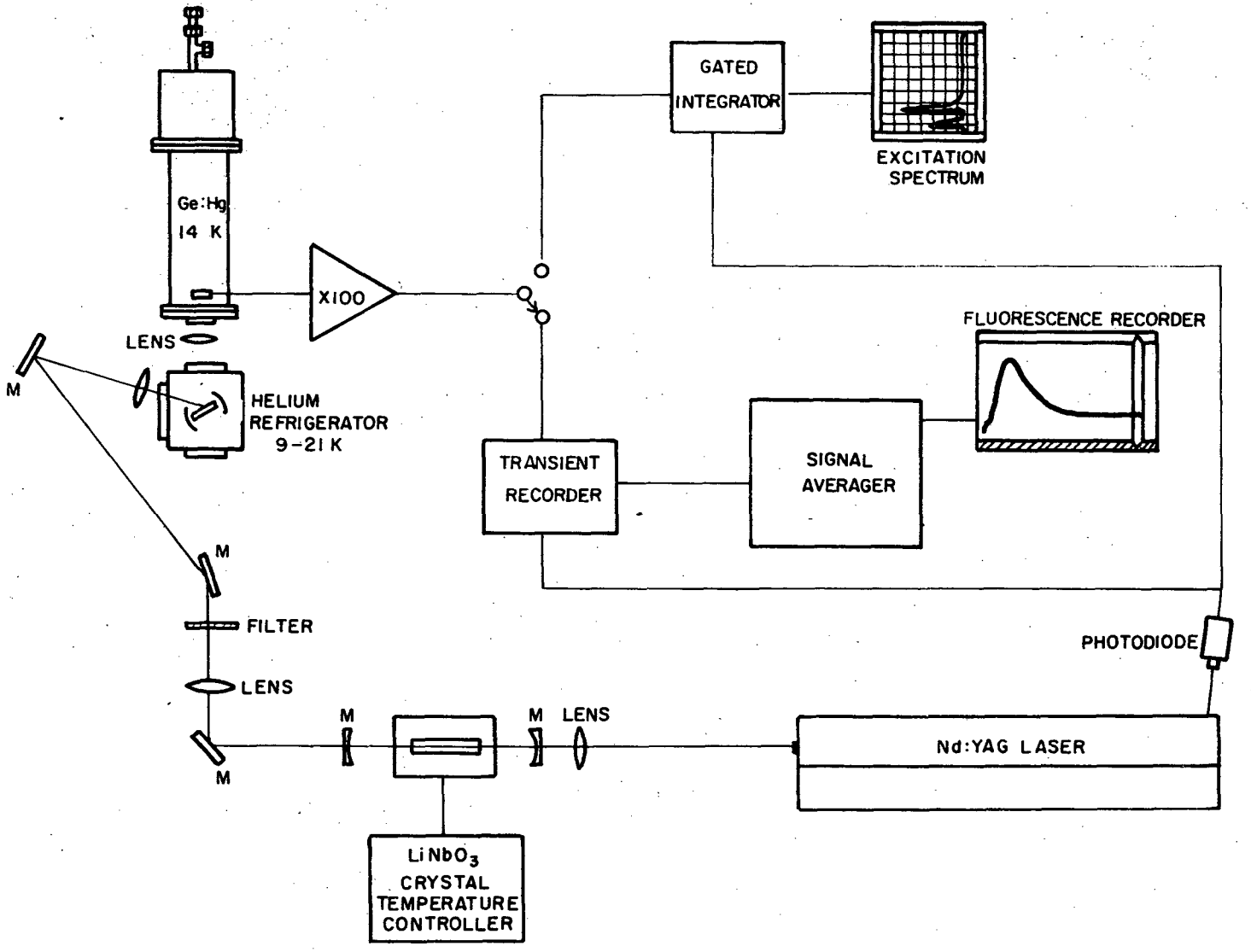

XBL 7710-10006

Fig. 1

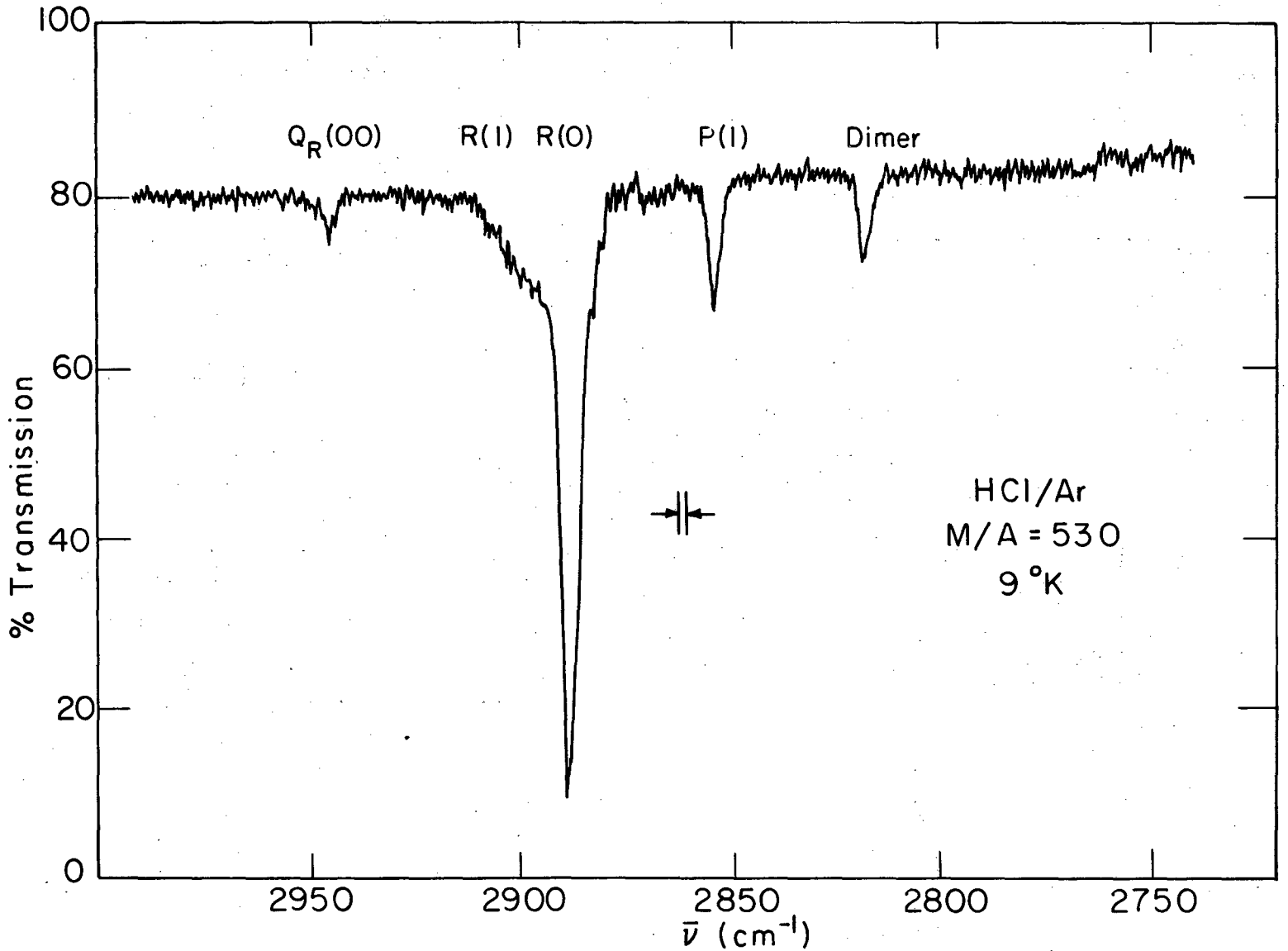

XBL 7710-10000

Fig. 2

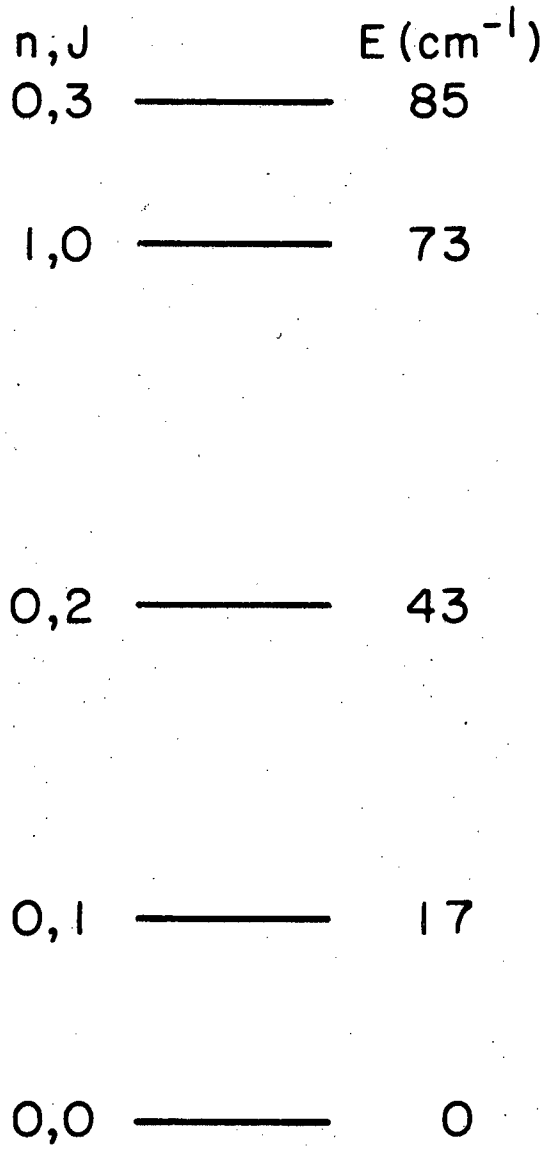

XBL 7710-6897

Fig. 3

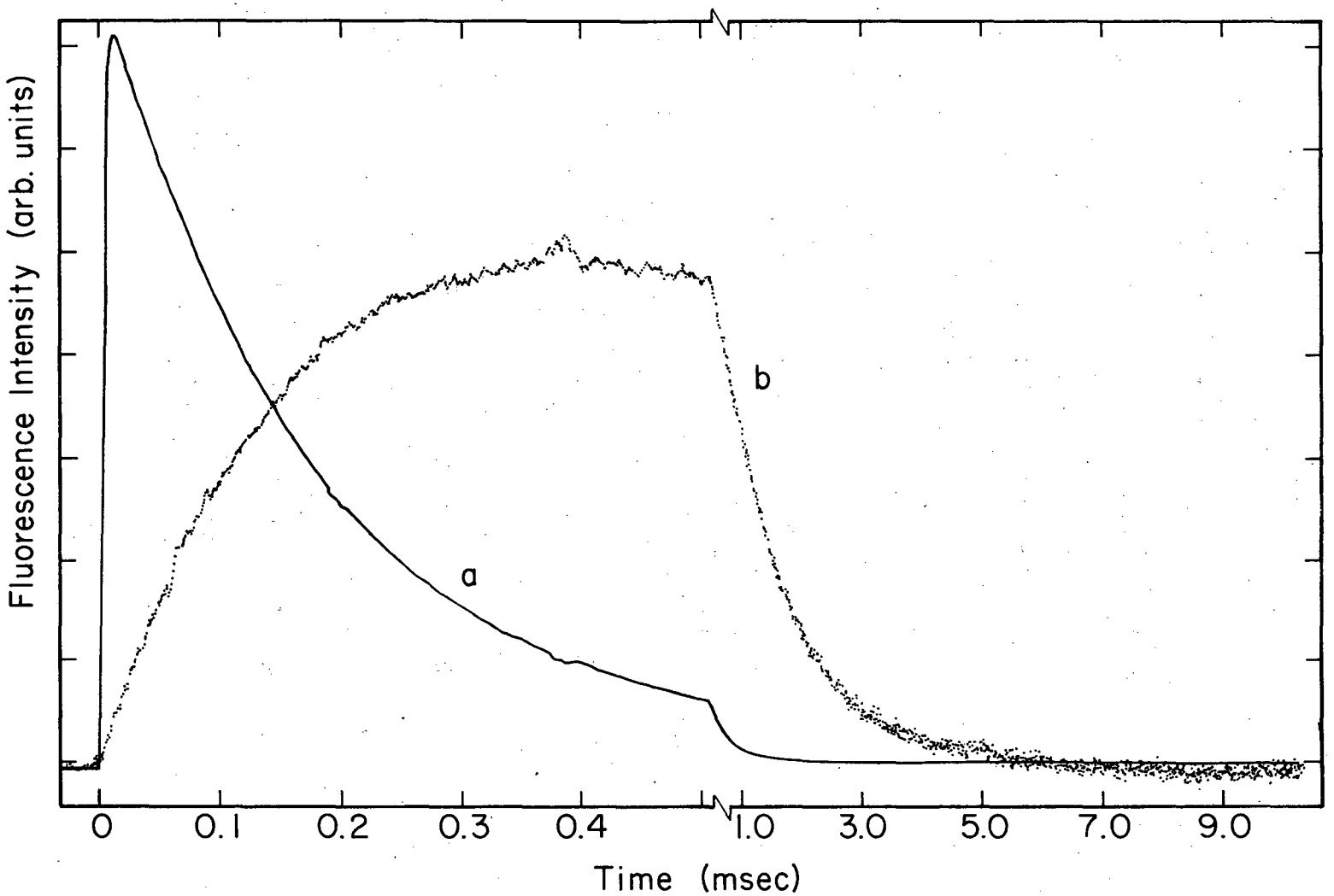

XBL 7710-10007

Fig. 4

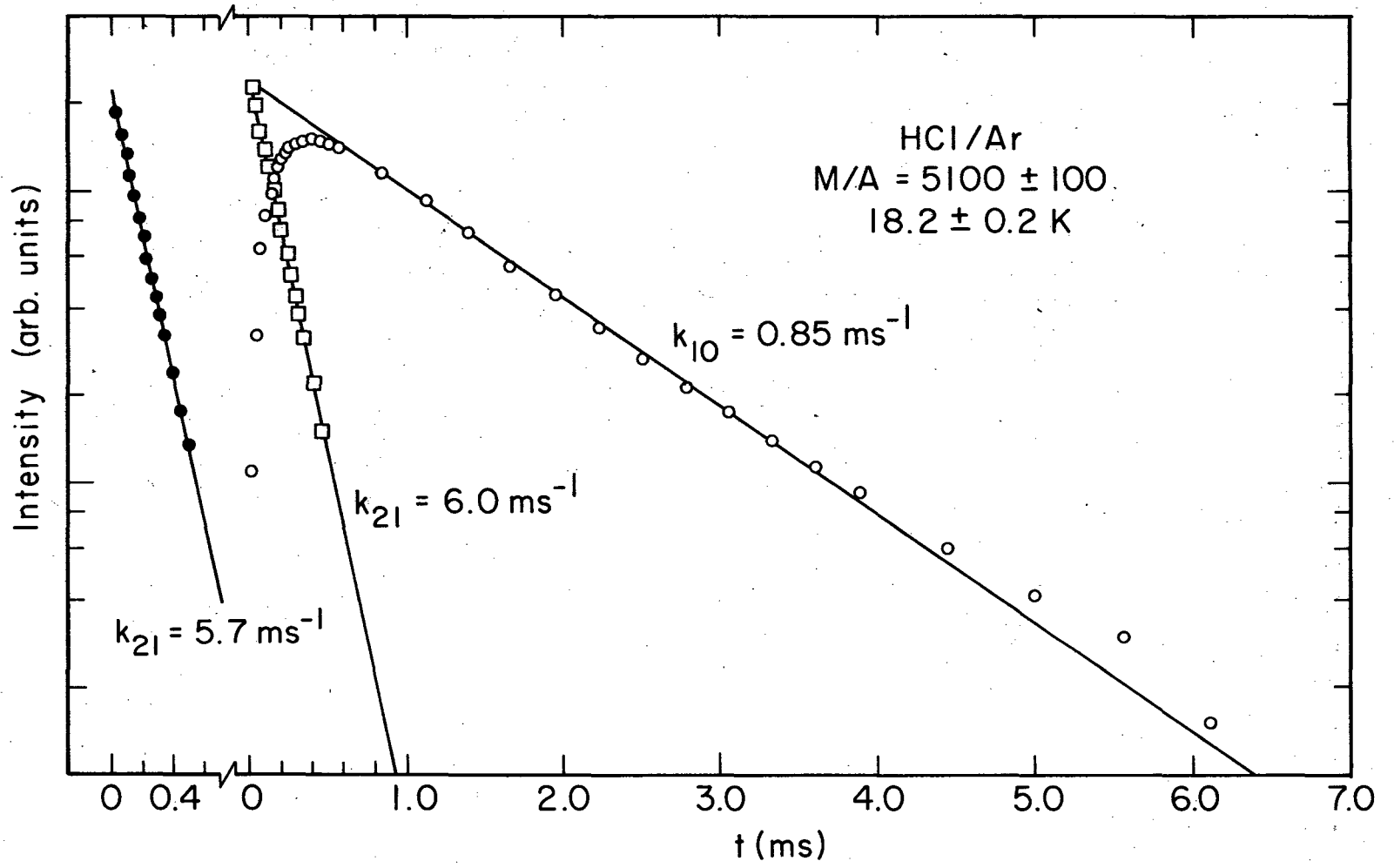

XBL 7711- 10362

Fig. 5

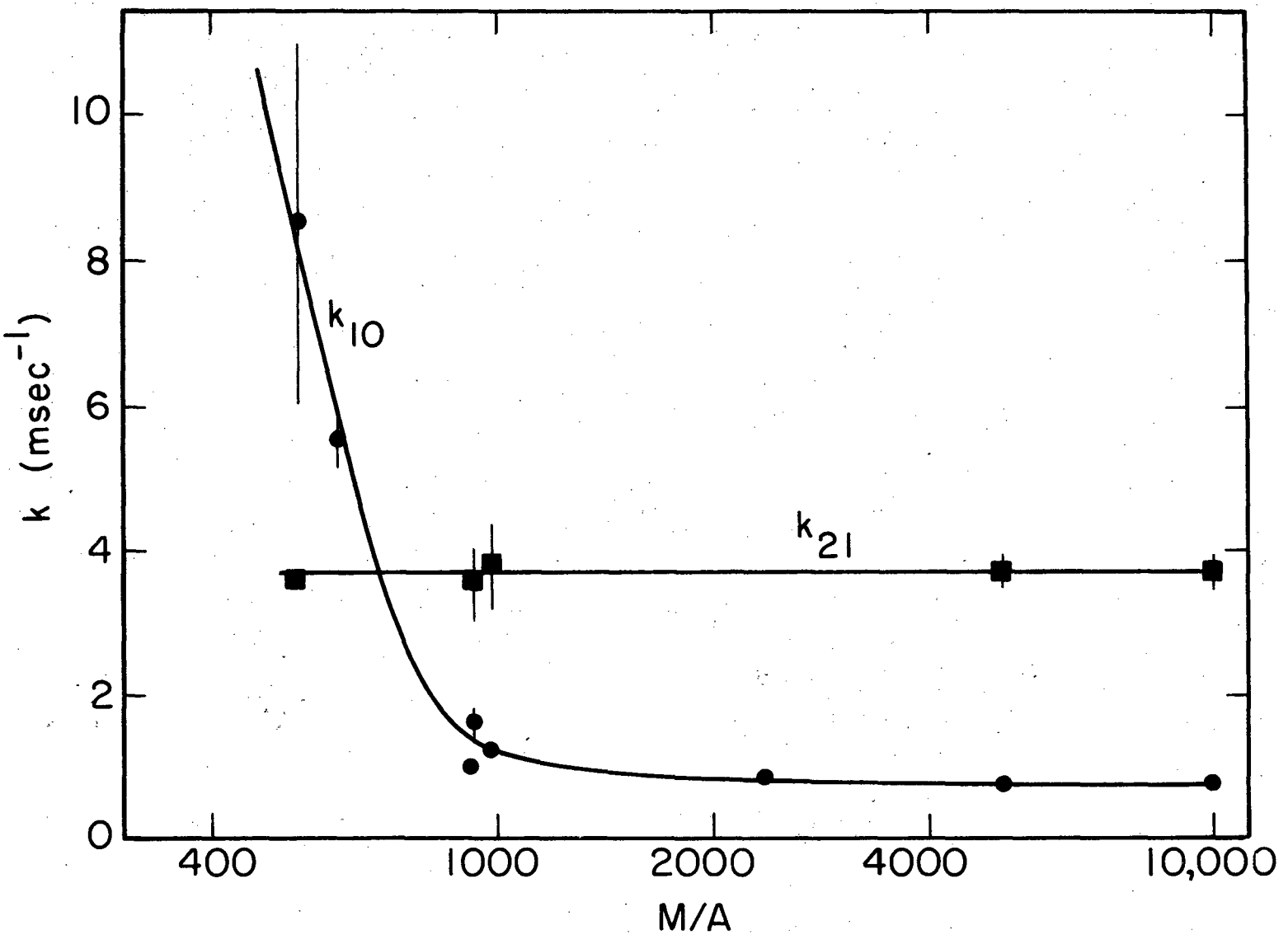

XBL 7710-10004

Fig. 6

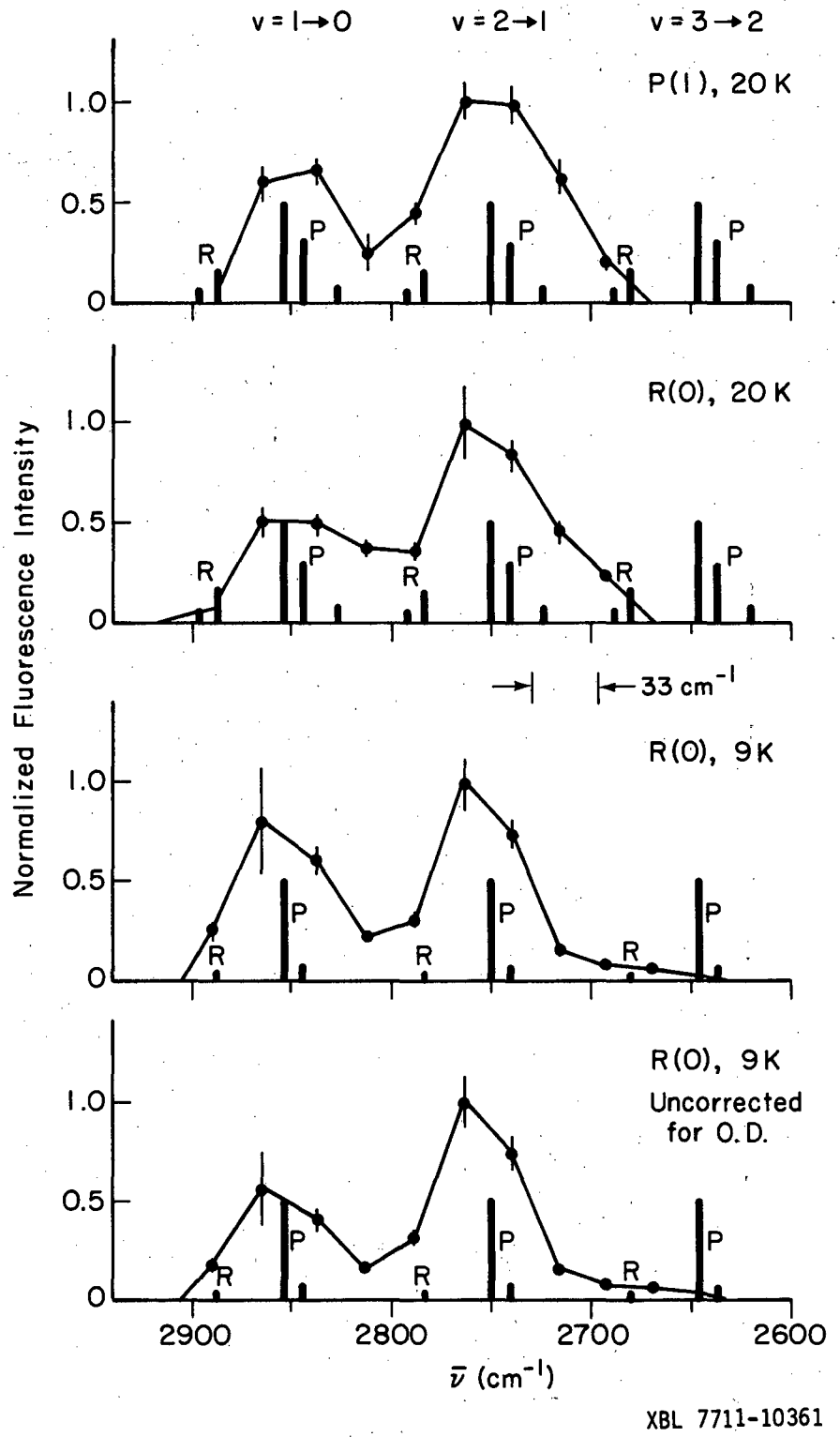
v = 1→0
v = 2→1
v = 3→2
P(1), 20 K
R(0), 20 K
R(0), 9 K
R(0), 9 K
Uncorrected
for O.D.
33 cm⁻¹
Normalized Fluorescence Intensity
1.0
0.5
0
R
P
2900
2800
2700
2600
ν̄ (cm⁻¹)
XBL 7711-10361

Fig. 7

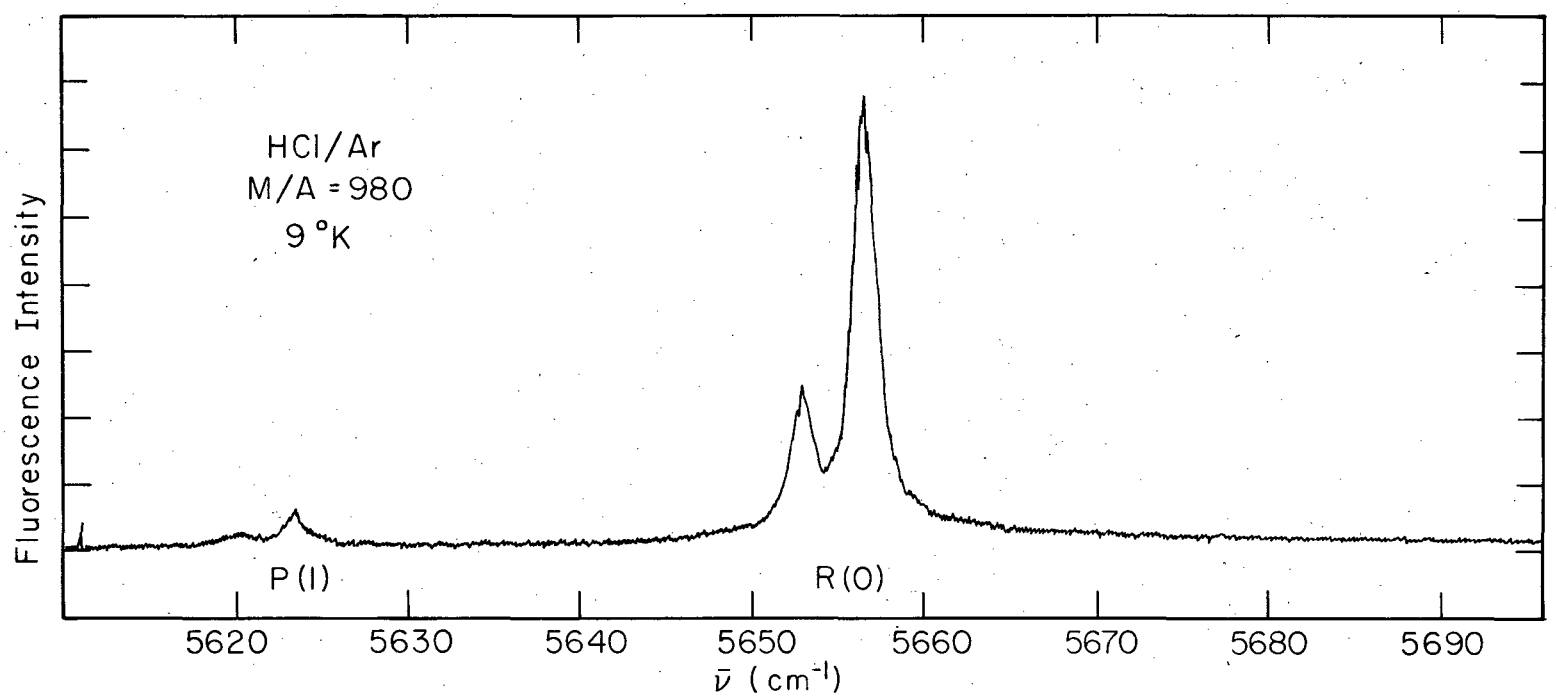

XBL 7710-6898

Fig. 8

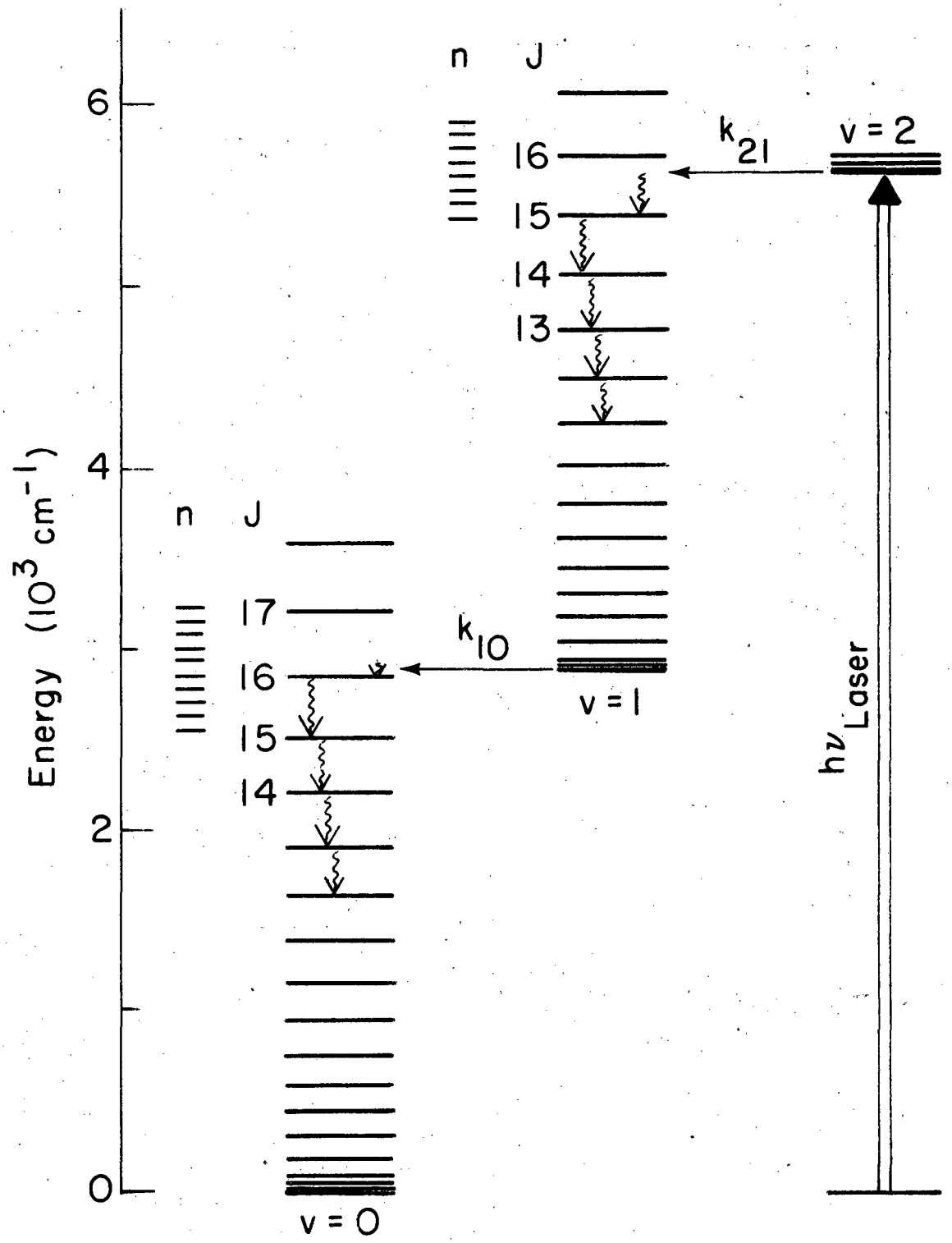

Fig. 9

XBL 7710-10002

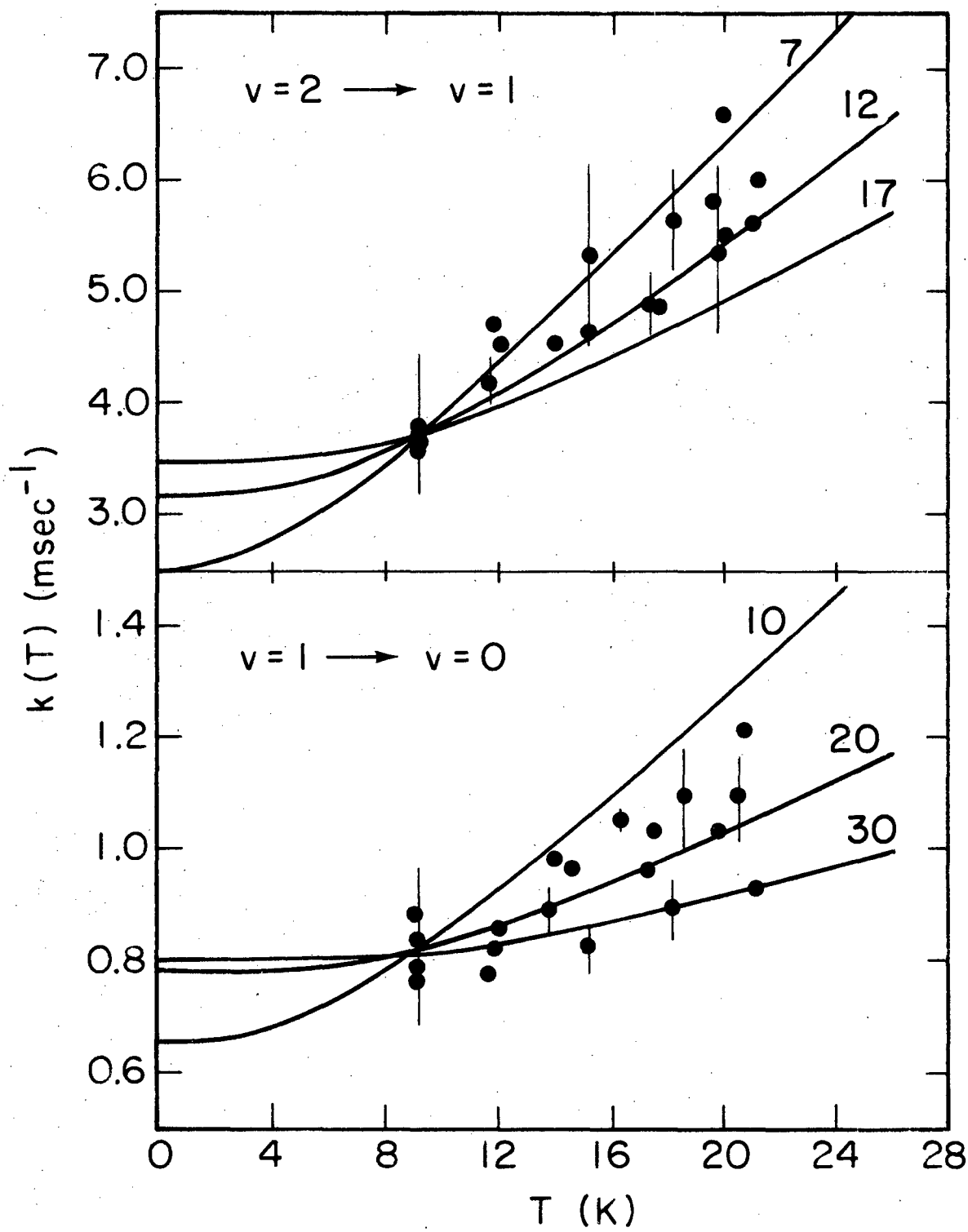

XBL 7710-6896

Fig. 10

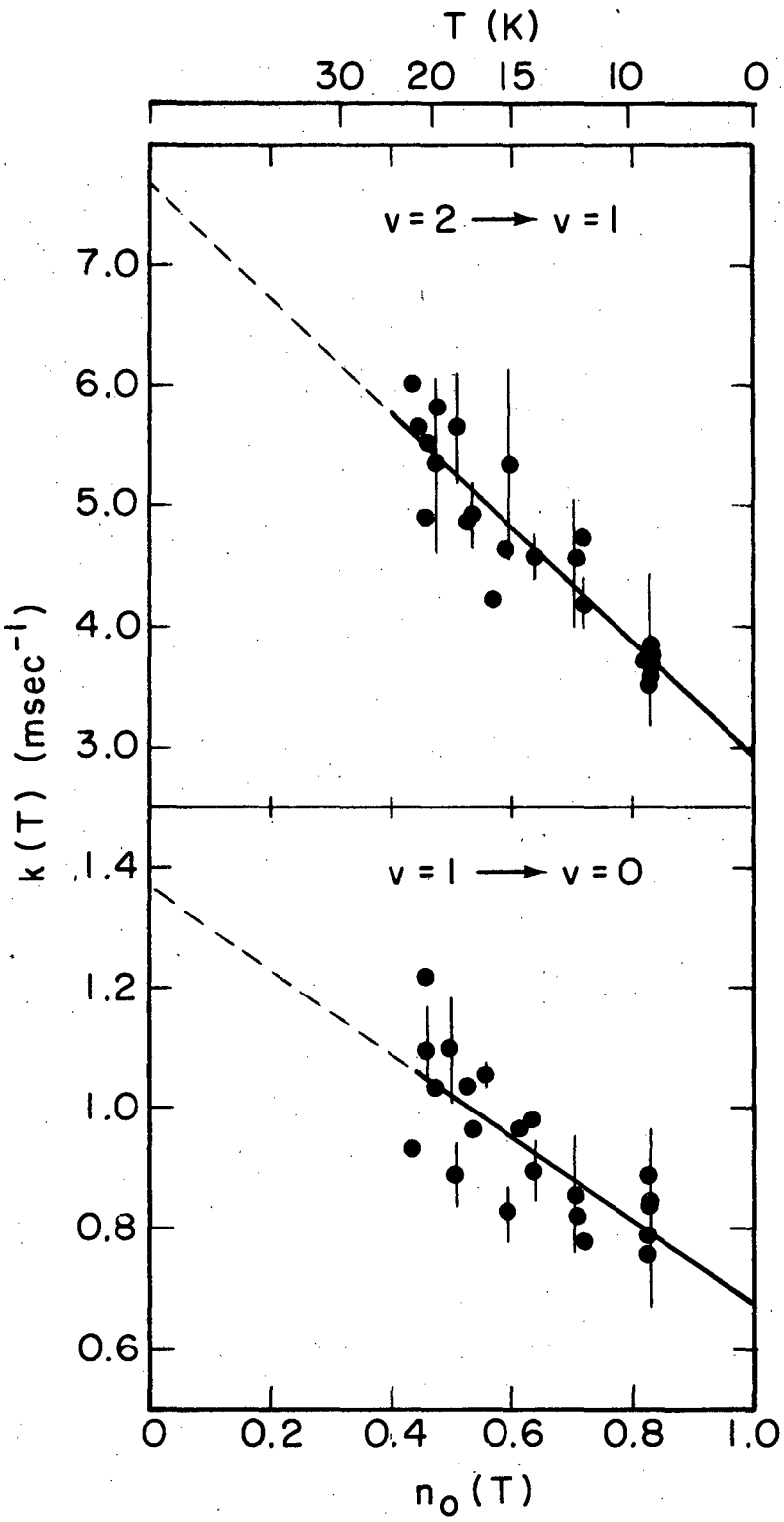

XBL 7710-10003

Fig. 11

U.S.GPO:1978-789-158/(F)14

This report was done with support from the Department of Energy. Any conclusions or opinions expressed in this report represent solely those of the author(s) and not necessarily those of The Regents of the University of California, the Lawrence Berkeley Laboratory or the Department of Energy.

TECHNICAL INFORMATION DEPARTMENT
LAWRENCE BERKELEY LABORATORY
UNIVERSITY OF CALIFORNIA
BERKELEY, CALIFORNIA 94720